Paper for: **IAEA Technical Meeting on Compatibility between Coolants and Materials for Fusion Facilities and Advanced Fission Reactors**

Title: **Parametric study of ITER main Primary Heat Transfer System coolant chemistry and operational parameters using OSCAR-Fusion v1.4.a code**

Authors: D. Carloni[1], F. Dacquait[2], F. Broutin[2], L. Di Pace[3], T. Shimaoka[1], F. Javier[1], Y. Le Tonqueze[1]

1 ITER Organization, Route de Vinon-sur-Verdon, F-13115 Saint-Paul Lez Durance, France

2 CEA, DES, IRESNE, DTN, Cadarache, F-13108 Saint-Paul lez Durance, France

3 RINA Consulting CSM, 00128 Castel Romano (RM), Italy

Abstract

The ITER main Primary Heat Transfer System, the Integrated Blanket, ELMs and Divertor loop (IBED PHTS), provides two key functions for the in-vessel components installed inside the vacuum chamber:

- active cooling to effectively remove most of the heat coming from the D-T plasma and
- high temperature baking to purge the in-vessel components from tritium and other impurities.

The design of the IBED loop foresees water as fluid: hence, corrosion products will accumulate in the circuit because of the interaction of the fluid with the wet surfaces of the circuit; in addition, the neutron flux generated by the D-T plasma will activate the corrosion products and the base metal as well.

Consequently, activated corrosion products will contaminate piping and associated equipment inside and outside of the bioshield, thus to represent a source term for both normal operation and accidental situations safety studies.

The Radiological Beryllium Safety and Environmental (RBSE) group within ITER Safety and Quality department launched a parametric studies campaign on the IBED PHTS water chemistry with the purpose to assess the influence of the water properties on the generation of corrosion products, the spreading of the activated ones and consequent overall contamination of the loop.
The focus was on the water chemistry properties, notably the pH and the hydrogen and lithium concentration during plasma and baking operations. Additionally, Chemical and Volume Control System (CVCS) and baking loop operational parameters (i.e. flow rate and temperatures) were also investigated.

These studies used OSCAR-Fusion v1.4.a to assess the impact of water chemistry and operational parameters on the inventory of activated corrosion products in the coolant and on the walls of the IBED loop.
The paper will describe the rationale for the parametric studies and discuss the results obtained from OSCAR-Fusion calculations. It will also provide some recommendations enabling a reduction of the ACP inventory and hence the impact in terms of Occupational Radiological Exposure.

Table of Contents

Scope

This report focus on the ACPs inventory within the IBED loop during dwell, plasma operation, baking and cold shutdown; draining and drying operation are outside the scope of this work. Material activation during Fusion Plasma Operation (FPO) campaigns has been calculated in [75TC8J], considering also deactivation rates for some isotopes.

The simulation of material activation during Pre-FPO (PFPO) is not treated, although scaling factor from [7VALZX] allow conservative estimates of ACPs inventory at the end of PFPO campaigns.

Definitions

ACPs	Activated Corrosion Products
BLK	Blanket
BM	Blanket Module
CP	Corrosion Products
CS	Cold Stand-by
CVCS	Chemical and Volume Control System
DIV	Divertor
ELMs	Edge Localised Modes
EMECC	Ensemble des Mesures et d'Etude de la Contamination des Circuits
EoL	End of Life
FPO	Fusion Power Operation
FW	First Wall
GUI	Graphical User Interface
HV	Hypervapotron
HX	Heat Exchanger
IBED	Integrated Blanket ELMs and Divertor
IVCs	In-Vessel Coils
OSCAR	tOol for Simulating ContAmination in Reactors
PFPO	Pre Fusion Power Operation
PHTS	Primary Heat Transfer System
PWR	Pressurized Water Reactor
TCWS	Tokamak Cooling Water System
VV	Vacuum Vessel

References

IDM N.	Title
[27ZRW8]	Project Requirements (PR) (27ZRW8 v6.3/E) (current)
[2823A2]	D. Lioce et al. SRD-26-PH, -CV, -DR, -DY, -SA (TCWS) from DOORS (2823A2 v6.4/E)
[2F6J4N]	Technical Specification for IBED Main Heat Exchanger Structural Analysis (2F6J4N v3.0)
[39CFJC]	ACP contamination in several TCWS IBED-PHTS locations - normal maintenance (39CFJC v1.0)
[3ZR2NC]	Preliminary Safety Report (RPrS) (3ZR2NC v3.0) (current)
[632JT5]	Engineering support for TCWS ACPs assessment (632JT5 v2.0)
[6W87VQ]	Neutron spectrum (TRIPOLI 315) in Be layer of FW of BLK15 S02 (C-model R181031 with heterogeneous BLK15 S02; TMP and MT considered) in the nominal plasma shot of 500MW fusion power. (6W87VQ v2.1)
[75TC8J]	Production of the isotopes to be considered as the dominant ACP contributors to the dose equivalent rate (7T5C8J v1.3)
[7URCSP]	D. Carloni, Engineering support for TCWS ACPs assessment - 1st deliverable - Review, Update and Validation of the 2021 OSCAR input, 7URCSP v1.1, 2021
[7VALZX]	Scaling factors for conservative evaluation of the radiation conditions in FP/PFPO (7VALZX v1.1)
[87D6BT]	D. Carloni et al. WP-A-3: Validation of the OSCAR input and its results (Engineering support for TCWS ACPs assessment - 2nd Deliverable) (87D6BT v1.2)
[89DGN3]	Deviation Request - TCWS - Cobalt Content Flanges (89DGN3 v1.0)
[8E6SZW]	NIE final ALARA/ORE status end of 2022 (8E6SZW v1.5)
[8HMD4L]	Technical Report CEA/DEN - OSCAR-Fusion V1.3 - Description of the physical models
[8L64V5]	Memorandum - Estimation of likely temperature cycles for PFPO and FPO (8L64V5 v1.0)
[8L76F7]	Overview of experimental PFPO and FPO campaigns (8L76F7 v1.2) (current)
[8M2NJK]	F. Dacquait et al., Modelling of the contamination transfer in nuclear reactors: The OSCAR code Applications to SFR and ITER, 1st IAEA Workshop on Challenges for Coolants in Fast Neutron Spectrum Systems, Vienna (Austria), 5-7 July 2017, TECDOC-1912, 2020
[8M2QAP]	F. Dacquait et al., Simulation of Co-60 uptake on stainless steel and alloy 690 using the OSCAR v1.4 code integrating an advanced dissolution-precipitation model. Nuclear Engineering and Design, 405, 112190 (2023). https://doi.org/10.1016/j.nucengdes.2023.112190
[8XUD54]	F. Broutin & F. Dacquait. OSCAR-Fusion v1.4.a - Comparison with OSCAR-Fusion V1.3. CEA/DES/IRESNE/DTN/SMTA/LMCT/NT/DO/2023-09
[93LM97]	V. Belous et al., Assessment of the corrosion behaviour of structural materials in the water coolant of ITER. Journal of Nuclear Materials, 258-263, 351-356 (1998)
[9AT83Q]	F. Dacquait et al., Status of primary system contamination in French PWRs, Int. Conf. on Water chemistry in nuclear reactors systems, NPC 2004, San Francisco (USA).
[9ATZVR]	R. Eimecke & S. Anthoni. Ensemble de Mesure et d'Etude de la Contamination des Circuits (EMECC). 7th International Conference on Radiation Shielding, Bournemouth (England), September 1988.
[9DTBX9]	F. Dacquait & F. Broutin. Validation elements for OSCAR-Fusion v1.4.a. CEA/DES/IRESNE/DTN/SMTA/LMCT/NT/DO/2023-10
[9FLK4Z]	S. Wikman et al. Experimental Assessment of Erosion Corrosion Parameters of Copper Alloys and Copper to Steel Joints at ITER Operational Conditions, 2013.
[9FLNFB]	IAEA Technical Report Series No.347 – COOLANTTECHNOLOGY OF WATER COOLED REACTORS: AN OVERVIEW
[Appendix M]	Private mail from PBS 17 to RBSE – T. Hirai on 01/07/2022 (appendix M)
[RWBRH3]	IBED-PHTS Input data for system code analyses (RWBRH3 v4.3) (current)
[WLS6FF]	Neutron production in FPO according ITER Research Plan (wls6ff v1.1) (current)
[WU8LSB]	Divertor model input data for ACP evaluation with OSCAR for IBED (ITER_D_WU8LSB v1.1)

[WU9YPS]	Blanket model input data for ACP evaluation with OSCAR for IBED (ITER_D_WU9YPS v1.1)
[WVJMH4]	WP3.5.0a IBED CVCS. Validation of letdown flow (WVJMH4 v3.0)
[X83W55]	IBED ex-vessel loop model input data for ACP evaluation with OSCAR (ITER_D_X83W55 v1.0)
[XNXW3N]	Baseline ACP assumptions and calculations (XNXW3N v1.0) (current)
[XQ7LQV]	Melcor technical specification for models update, maintenance services and SD support - task 3 (XQ7LQV v1.0)

1 Brief Description of the IBED loop

ITER in-vessel components require active cooling to effectively transfer the heat generated by the products of the D-T fusion reaction i.e. mainly alpha particles and neutrons. The main in-vessel components are the First Wall-Blanket (FW-BLK) and the Divertor (DIV).
The FW-BLK consists of 440 modules covering the equatorial and upper regions of the Vacuum Vessel; its main functions are enabling the heat removal from the plasma and providing adequate neutron shielding to the VV and the superconducting magnets.
The divertor consists of 54 cassettes occupying the lower region of the Vacuum Vessel; it withstands high heat loads coming from the plasma and enables to exhaust gas and impurities from the vacuum chamber.
Additional in-vessel components are the In-Vessel Coils (IVCs), mounted on the VV surface right behind the FW-BLK, the Diagnostics and Auxiliary Heating Systems installed in the equatorial and upper ports.

The Integrated Blanket ELMs and Divertor (IBED) Primary Heat Transfer System (PHTS) is designed to provide cooling to all the above mentioned in-vessel components, adequately removing the heat coming from the plasma and hence avoiding undue high temperature transients. This system enables also water and gas baking operation to purge tritium and other impurities from the IVCs through its connection to the baking circuit, i.e. a circuit capable to heat-up the water up to 240 °C. A CVCS circuit is connected to the PHTS through two linear headers to remove ions and particles in the coolant through resin beds and mechanical filters respectively.

The IBED loop considered in this work is then the sum of all the above mentioned systems providing a barrier to both water and ACPs release: the figure below shows a simplified flow diagram of the IBED loop with the details of the ratio of the total flow rate in different branches of the circuit during both dwell/burn and baking operations.

Additional auxiliary systems of the IBED PHTS are the draining and drying circuit, not considered for the present study since OSCAR cannot simulate the emptying of one circuit into another. However, the transfer of ACPs to the drain tanks through the draining connections can and shall be addressed for both maintenance and accidental scenario; the results in terms of ACPs concentration in the coolant shown in following section 8 can enable such estimation.

Figure 1 below shows the IBED loop sub-division in 4 areas:

- In-flux regions, i.e. the regions of the loop within the bio-shield activated by the neutrons (inside the red rectangle in figure)
- Out-of-flux regions, i.e. portions of the IBED loop belonging to the PHTS outside the bioshield, including piping, valves and main HXs
- The baking circuit connected in parallel to the PHTS (inside the orange rectangle in figure)
- The CVCS circuit connected in parallel to the PHTS (inside the green rectangle in figure)

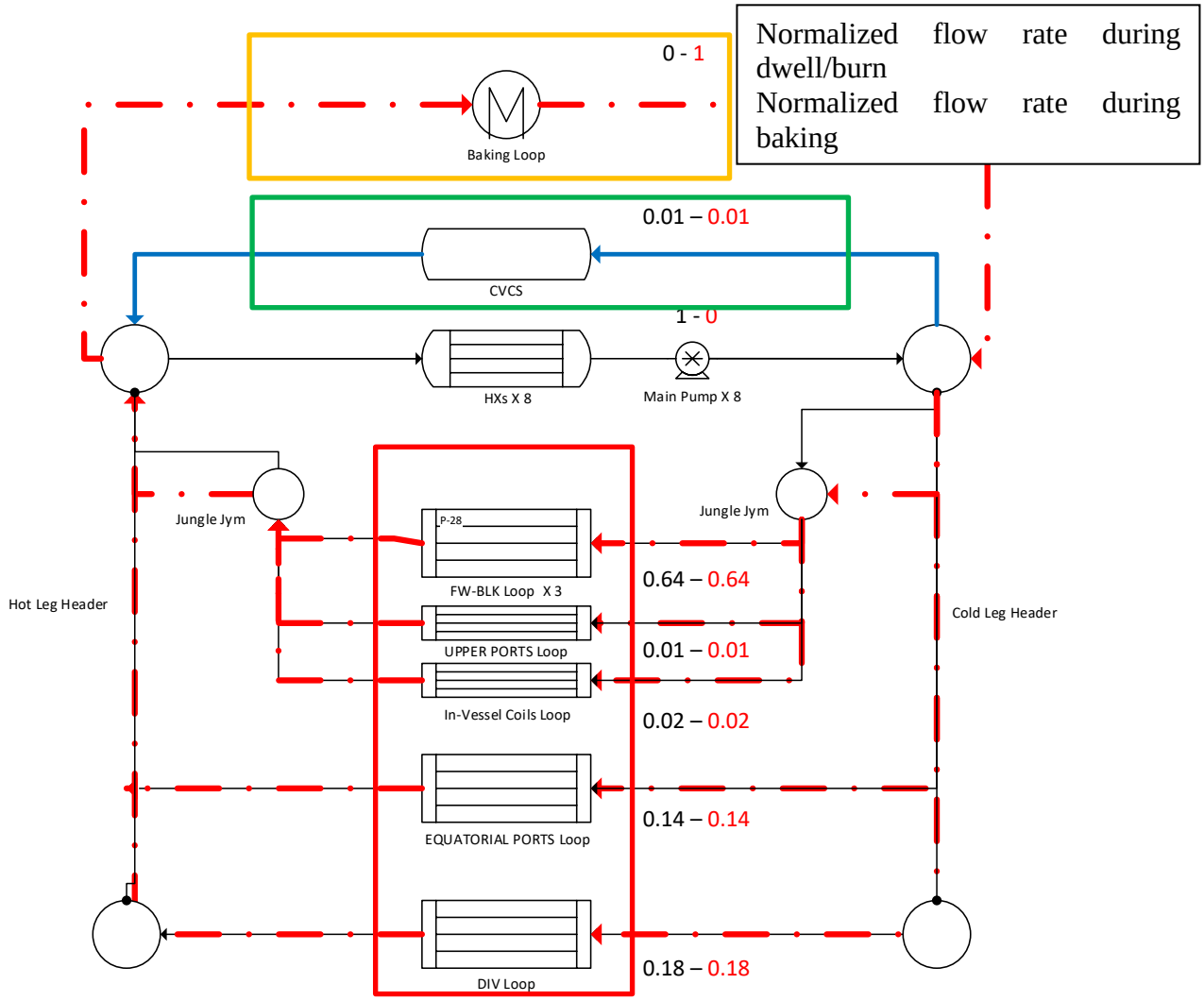

Figure 1 – IBED loop simplified flow diagram; the red dotted lines represent the branches of the circuit in which 240 °C water circulates during baking

It is also worth to remind that IBED is the main system of the TCWS, both in terms of coolant inventory, flow rate and power to be transferred to the heat rejection system. It is a rather large and complex assembly of piping and cooling equipment (e.g. valves, heat exchangers) containing activated coolant and corrosion products thus to represent an unprecedented challenge in terms of inspection and maintenance activities [8E6SZW].
Therefore, the ACPs assessment for IBED is one of the main input for the overall safety performances of the ITER project.

2 OSCAR-Fusion v1.4 code

2.1 Description of OSCAR-Fusion

The OSCAR-Fusion code is the TCWS PHTS version of the OSCAR code initially developed for the PWR reactor cooling system [8M2NJK]. Since the coolant used in the PHTSs and PWRs is the same and the main differences concern the materials (presence of copper alloy) and the neutron flux (higher neutron flux), the ACP transfer modelling in the OSCAR-Fusion code is identical to that in the OSCAR code. Therefore, the OSCAR-Fusion code adopts the same control volume approach for modelling, which can be summarized as follows:

- The systems are divided into discrete control volumes or regions based on their geometric, thermal-hydraulic, neutronic, material, and operational characteristics;
- Each control volume can encompass six media: metal, inner oxide, outer oxide/deposit, particles, ions, and filter (including ion exchange resins and particle filters);
- The code considers the following elements: Cr, Mn, Fe, Co, Ni, Zn, Zr, Ag, Sb and Cu along with their respective radioisotopes;
- For each isotope (both stable and radioactive) in each medium of each region, a system of mass balance equations is solved using the following equation:

$$\partial m^i / \partial t = \sum_{sources} J^i_{transfer} - \sum_{sinks} J^i_{transfer}$$

where m^i is the mass of isotope i in a given medium [kg], t the time [s] and $J^i_{transfer}$ a transfer mass rate of isotope i between 2 media or 2 regions or 2 isotopes [kg.s^{-1}].

The main transfer mechanisms accounted for in the code include corrosion-release, dissolution, precipitation, erosion, deposition, convection, purification, activation, and radioactive decay (see Figure 2).

The dissolution-precipitation model was enhanced in version 1.4, enabling OSCAR to more accurately calculate the incorporation of minor species (e.g., ^{60}Co) into oxides (see [8M2QAP] for a detailed description of this new model and the other main ones).

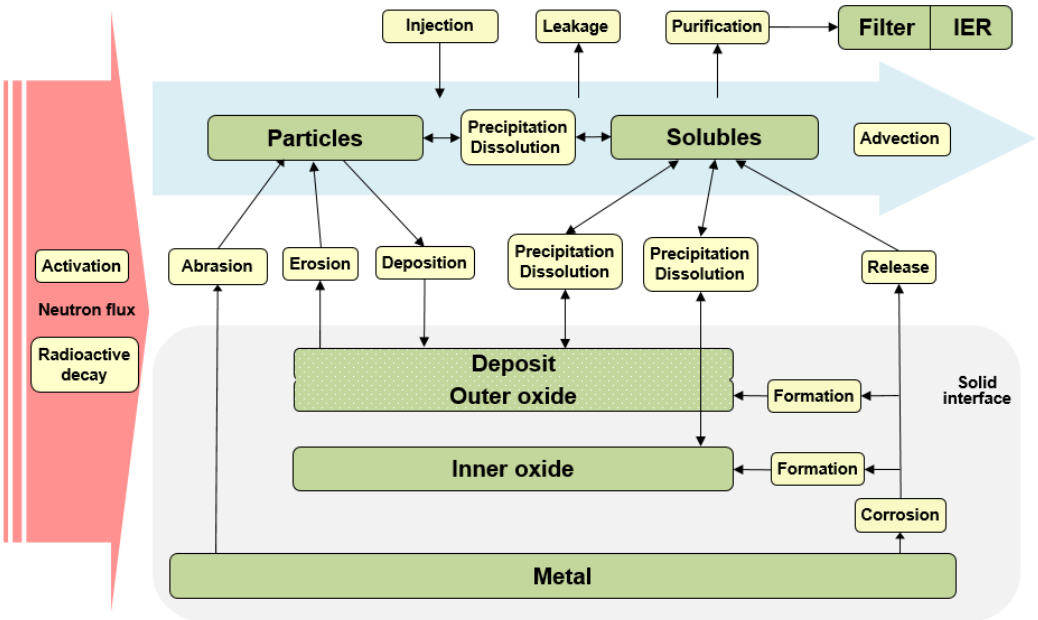

Figure 2: Mass transfer mechanisms included in the OSCAR v1.4 code (figure from [8M2QAP])

In past analyses ([XNXW3N], [39CFJC] [XQ7LQV]) OSCAR version 1.3 has been used, whereas IO has been using OSCAR Fusion v.1.4a since June 2022[7URCSP].

2.2 Differences between OSCAR-Fusion v1.4 and v1.3

2.2.1 Modelling improvements

Some of the main improvements of OSCAR v1.4 compared to OSCAR v1.3 are summarized below:

- Definition of an isotopic dissolution and precipitation mechanism,
- Dissolution rates as a function of pH, p_{H2}, and p_{O2},
- Homogeneous precipitation rate as a function of the nucleation site surface,
- Ability to determine equilibrium concentrations based on solid phase stability,
- Ability to add a particle or agglomerate entrainment mechanism through dissolution,
- Ability to manage H_2 and O_2 concentrations by region,
- Consideration of the effect of Zn on corrosion rates (MOOREA law),
- Improved simulation of nucleate boiling by considering an Agglomerates medium,
- Introduction of water activation products ^{16}N and ^{41}Ar,
- Ability to add a leakage flow rate by region,
- Ability to add a decontamination factor by region (i.e. the possibility to simulate the removal of contaminant in the form of deposit and/or inner oxide from specific regions)

The impact of these changes on the results of OSCAR-Fusion is presented in [8XUD54].

2.2.2 GUI improvements

The following specific improvements have been or will be made to the input GUI of OSCAR-Fusion v1.4 to meet the needs of ITER:

- Ability to disable writing results at each period, resulting in reduced output file size and shorter run duration (done),
- Ability to disable temperature interpolation between two periods, simplifying the modelling of pulses (done),
- Simplification of the definition of operating parameters by allowing them to be repeated multiple times, reducing the size of input files and simplifying the modelling of pulses,
- Automatic calculation of fluid velocity based on flow rate, hydraulic diameter, and the number of sub-elements in a region, eliminating the need for a reference period,
- Automatic calculation of relaxation length (done),
- Introduction of two user modes: Standard user and Expert user (done) – Standard user mode prevent the user to modify some code parameters (e.g. corrosion laws, correction factors)
- Addition of values in labels for Time-Region indices,
- Improved management of the NUCLEO_OSCAR_Fusion.xml file, including a review of the definition of in-flux zones.

2.2.3 Differences in the parameters of the datasets

The main difference concerns the corrosion rates of SS and Cu alloy. For the calculations performed in the past [XNXW3N] [39CFJC], the MOOREA law was used for both SS and Cu. The MOOREA law is an empirical model that depends on the chemistry, temperature, material, manufacturing process and time. It was defined under PWR conditions for SS and Ni base

alloys. The model assumes an initial constant value for the first two months, followed by a gradual decrease over the next ten months, reaching a constant value thereafter. For SS, the MOOREA law depends on pH, saturation, temperature and time. For Cu alloy, it depends on saturation, temperature and time and assume the pH to be kept constant at 7.
To reduce conservatism and to use corrosion laws defined in ITER conditions [93LM97], OSCAR offers the possibility of using a power law for corrosion rate that consistently decreases over time instead of the constant corrosion rate after 1 year of operation of the MOOREA law (see section **Error! Reference source not found.**). The power law in OSCAR c an also depend on saturation and temperature, similar to the MOOREA law.
The differences in the other parameters of the datasets are indicated in [7URCSP], their impact being of the second order.

2.3 Validation of OSCAR-Fusion

While no operating experience (OPEX) exists for fusion reactors, the OSCAR-Fusion code benefits from the validation of the OSCAR code, which is based on a unique worldwide OPEX: the EMECC (Ensemble des Mesures et d'Etude de la Contamination des Circuits) expertise assessments. To date, approximately 430 campaigns of the γ surface activity measurements of the PWR primary and auxiliary systems have been conducted in 76 different units in France and abroad since 1971 using the EMECC system [9AT83Q]. In addition to the γ surface activities measured using the EMECC device [9ATZVR], the OSCAR results have been compared to other on-site measurements: volume activities and chemical element concentrations.
The validation of OSCAR encompasses a wide range of conditions including water temperatures ranging from 20 °C to 350 °C, both laminar and turbulent flow regimes, reducing and oxidizing environments, as well as alkaline and acidic conditions.
Validation elements for OSCAR-Fusion code are provided in [9DTBX9].

3 Reference case for parametric studies

This section compares the results obtained with OSCAR code to evaluate the impact of some parameters on the results and, more specifically, on the spreading of the contamination within the IBED loop.
The reference case is the input show in section 7.1.

3.1 Reference case

The reference case, i9, considers bespoken Cu alloy corrosion law derived from experimental data up to 250 °C reported in [9FLK4Z].

The operational scenario corresponds to the one described in [87D6BT] and reported hereafter. The operational scenario for the OSCAR-Fusion model is based on the reports [8L76F7], [8L64V5] provided by the Operation section of ITER scientific division: such a scenario considers 2 PFPO campaigns and 8 FPO campaigns; it also specify that 30 days of baking operation will occur prior and after each campaign.

3.1.1 Pre-Fusion Power Operation

Two PFPO campaigns including baking are simulated in the first cycle; being the plasma power and consequent activation level considerably lower than during the FPO campaigns, here the focus is on predicting the thickness in the deposit and inner oxide (primarily affected corrosion-release mechanism occurring during baking).
Therefore, the first cycle simulation relies on a simplified approach: constant temperature (70 °C during PFPO and 240 °C during baking) and no activation of the materials.
The very first day of operation is simulated as a "zero power" burn (i.e. no activation in the in-flux regions), followed by 29 days of baking to correctly initialize the calculation.[1]

Table 1: PFPO scenario

Mode	Duration [days]	Comment
Circuit Initialization		
Burn	1	"Zero Power" to initialize the calculation (no activation)
PFPO 1		
Baking	29	
Dwell	540	
Baking	30	
Cold-shutdown	0	In the real scenario 240 days of cold shutdown to allow assembly operation
PFPO 2		
Baking	30	
Dwell	630	

[1] The current version of OSCAR-Fusion requires a "reference period" [8HMD4L], i.e. a period to start the computational run by setting fluid velocities and wall and bulk temperatures in every regions of the model. The current reference period is the burn during the FPO cycle.

Mode	Duration [days]	Comment
Baking	30	
Cold-shutdown	0	In the real scenario 240 days of cold shutdown to allow assembly operation
TOTAL PFPO		
	1290	

3.1.2 FPO Plasma Operation

The overall FPO plasma operation is simulated through six identical FPO campaigns each one generating $5x10^{26}$ neutrons corresponding to an overall 4700 h of D-T plasma pulse duration and $3x10^{27}$ generated neutrons [27ZRW8].
The sum of the neutron generation during FPO 1, 2 and 3 corresponds to $5x10^{26}$ neutrons – this value correspond to the neutron generation in each subsequent FPO campaigns (i.e. FPO 4-8. i.e.) [27ZRW8], [WLS6FF]; to reduce the computational time and simplify the model, the first three FPO campaigns are grouped in a single one.

Table 2: FPO Scenario

Mode	Duration [s]	Comment
1 day of D-T Plasma operation		
Burn	8000	500 MW plasma shot lasting 500 seconds 16 shots per day [8L76F7], [8L64V5]
Dwell	78400	Including Night Shift
1 DT session		
Dwell	9.98	14 days plasma session from [S7T73E] STM is simulated as dwell time
Burn	1.02	
STM	3	
1 FPO		
Baking	30	
Dwell	319.4	1 FPO simulating 32 sessions, i.e. 16 months of operation
Burn	32.6	
STM	96	
Baking	30	
Total 1 FPO	448+60= **508**	At the end of each FPO an 8 months cold-shutdown phase, is considered
TOTAL 6 FPO cycles [Days]		
Burn	**Dwell**	**Baking**	**Shutdown**
196 (4700 h)	**1916+ 576 (STM)**	**360**	**1200+12 (only for FPOs)**

At the end of the last FPO campaign, additional 12 days of cold shutdown are simulated to track down the evolution of the ACPs due to natural decay after shutdown.
Hence the overall duration of the simulation amount to 5500 days, corresponding to approximately 15 years of *continual* operation.

3.1.3 Period parameters used in OSCAR

The thermal hydraulic parameters of the IBED PHTS have been kept identical to the ones reported in [XNXW3N] with the exception of the 0.5 ppm of Lithium injection during the baking operation, as shown in the table below:

Table 3: Thermal-hydraulic parameters during the different operational phases

Phase	Coolant Temperature [°C]	Flow Rate [kg/s]	Coolant Pressure [bar]	Power Fraction	Li [ppm]
PFPO					
Dwell	70	4920	40	0	0
Baking	240	516	45	0	0.5
FPO					
Burn	140 hot leg 70 cold leg	4920	40	1	0
Dwell	70	4920	40	0	0
Baking	240	516	45	0	0.5

3.2 List of radioisotopes

Among all the elements exposed to the neutron flux, only the ones transported out-side of the bioshield can be defined as relevant; similarly among the many reaction rates occurring in the under-flux materials, only the ones contributing to the activity or to the dose due to ACPs exposure can be selected. This results in the selection of six elements: Co, Cr, Cu, Fe, Mn, Ni and Zr.

The list of isotopes considered for the reference case on the basis of elements selection is shown in the table below.

Table 4: Isotopes considered in OSCAR

Isotope	Contact Dose rate (from FISPACT) [Sv/hr/Bq]	Gamma emitter	1/2 life	ORE Relevant	Accidents Relevant	Radwaste relevant
Co-57	3.3E-11	Yes	272 d	No	Yes	No
Co-58	2.7E-10	Yes	71 d	Yes	Yes	No
Co-60	7.6E-10	Yes	5.3 y	Yes	Yes	Yes
Cr-51	1.1E-11	Yes	28 d	Yes	Yes	No
Cu-62	2.2E-10	Yes	585 s	No	Yes/No	No
Cu-64	4.8E-11	Yes	12.7 h	Yes/No	Yes	No
Cu-66	2.3E-11	Yes	306 s	No	Yes	No
Fe-55	7.3E-12	No (X)	2.7 y	No	Yes	Yes
Fe-59	3.6E-10	Yes	44 d	Yes	Yes	No
Mn-54	2.4E-10	Yes	312 d	Yes	Yes	No
Mn-56	5.4E-10	Yes	2.6 h	No	Yes	No
Ni-57	5.8E-10	Yes	1.5 d	Yes	Yes	No
Ni-59	1.0E-11	No (X)	76040 y	No	Yes/No	Yes
Ni-63	0.0E+00	No	101 y	No	Yes	Yes
Zr-93	0.0E+00	No	1.53E+06 y	No	No	Yes
Zr-95	1.8E-10	Yes	64 d	Yes	Yes	No

½ life < 1 day	1 day < ½ life < 1 year	1 year < ½ life < 10 years	100 years < ½ life

This list of isotopes can be further reduced in function of the study by considering additional selection criteria, like the relatively low half-life and/or negligible contribution to the dose; for instance isotopes with negligible contribution to the equivalent gamma dose and/or with relatively short half-life (i.e. < 1 day) can be excluded for ORE studies, as discussed in section 9.

3.3 Reaction rates assessment

The NUCLEO section of the OSCAR code contains the data related to the neutronic interactions with the materials under flux; it is broken down in three sub-sections:

- Element,
- Decay chain (*ChainePC*),
- Reaction Rates (*TauxDeReaction*).

The first two sub-sections are "standard" ones, i.e. they contain isotope-specific information such as type of element, mass number, natural abundance and, for radio-isotopes, decay type and time constant.
The Reaction rate sub-section shall be adapted to the type of study, providing the specific reaction rates for all the relevant isotopes. In particular, the radiological inventory variation during the entire simulation shall consider the contribution of both activation and de-activation rates, i.e. the disappearance of some relevant radionuclides by the interaction with the neutron flux or by natural decay, shall also be analysed.

To the purpose of providing an adequate input for NUCLEO, RBSE performed dedicated calculations to assess the neutron spectra during FPO in the First Wall – Blanket (FW-BLK) cooling channels [75TC8J] and hence calculated the reaction rates in different regions of a FW-BLK module [8E6SZW].

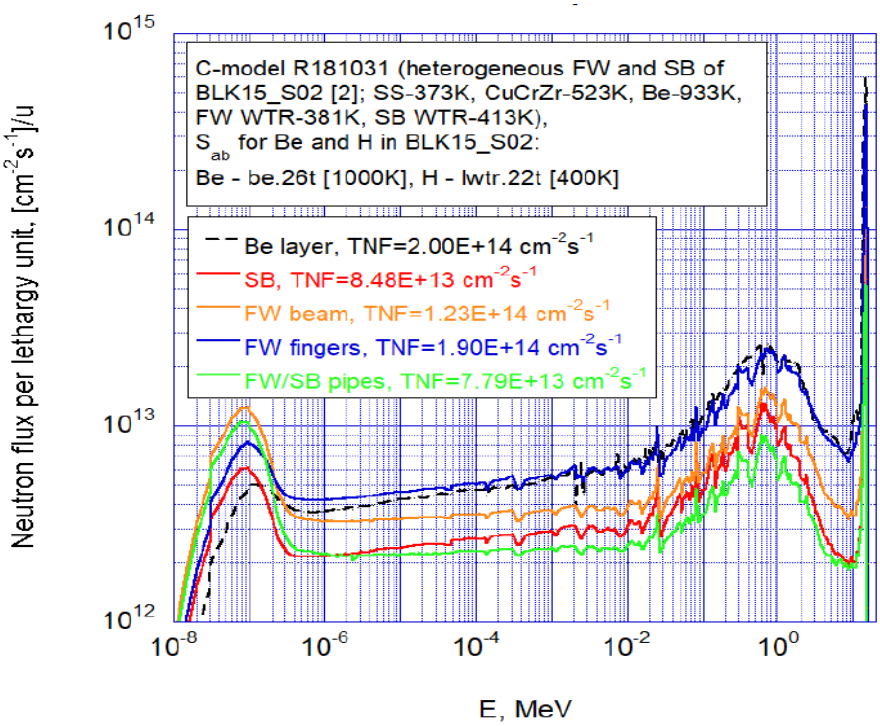

Figure 3: The neutron spectrum in TRIPOLI 315 energy group structure in the cooling channels in the first wall panel and in the shielding block of the blanket module BLK15_S02 at the flattop of the nominal plasma shot of the fusion power of 500MW [75TC8J]. The spectrum in the Beryllium layer has been added for the reference.

FISPACT code was used to provide the reaction rates for different materials and FW-BLK regions, thus to provide a good level of detail in terms of both isotopes activation and spatial distribution.

In addition, the disappearance of four radioactive isotopes (Co-58, Co-60, Cu-64 and Mn-56) were also investigated and the respective annihilation rates included in the reactions list.

As a result, the reaction rates lists were selected for OSCAR calculation; they are reported in Appendix **N (NUCLEO)**.

Simulation of activation of the materials during PFPO is not considered in the present work (an additional dedicated set of activation studies to provide input data for NUCLEO would be required); however, it is possible to conservatively extrapolate the activation at the end of each PFPO campaign on the basis of the ACPs inventory at the end of life and the scaling factors proposed in [7VALZX].

3.4 IBED loop regions and materials

The OSCAR-Fusion input model for the IBED loop used in past calculations and input documents ([XNXW3N], [39CFJC], [XQ7LQV] and [X83W55], [WU8LSB], [WU9YPS] respectively) has been updated on the basis of [RWBRH3] and [WVJMH4].

3.4.1 Regions

The IBED loop can be broken down in 4 areas:

- In-flux regions, i.e. the regions of the loop within the bio-shield activated by the neutrons,
- Out-of-flux regions, i.e. portions of the IBED loop belonging to the PHTS outside the bioshield,
- The baking circuit connected in parallel to the PHTS,
- The CVCS circuit connected in parallel to the PHTS.

Each area comprehends several regions, each region being defined in function of geometric (e.g. wet surface), thermohydraulics (e.g. temperature) and material (e.g. AISI316 or Copper, roughness) parameters.
The current version of the input has a total of 60 regions: 28 for the Out-of-flux, 26 for the in-flux, 3 for CVCS and 3 for the baking circuit; Appendix G gives details and reference on IDM of the data used for each region in the OSCAR input.

Figure 4 gives an overall view of the IBED loop model elaborated through the OSCAR Graphical User Interface (GUI); a magnified version of the GUI model is reported in Appendix I.

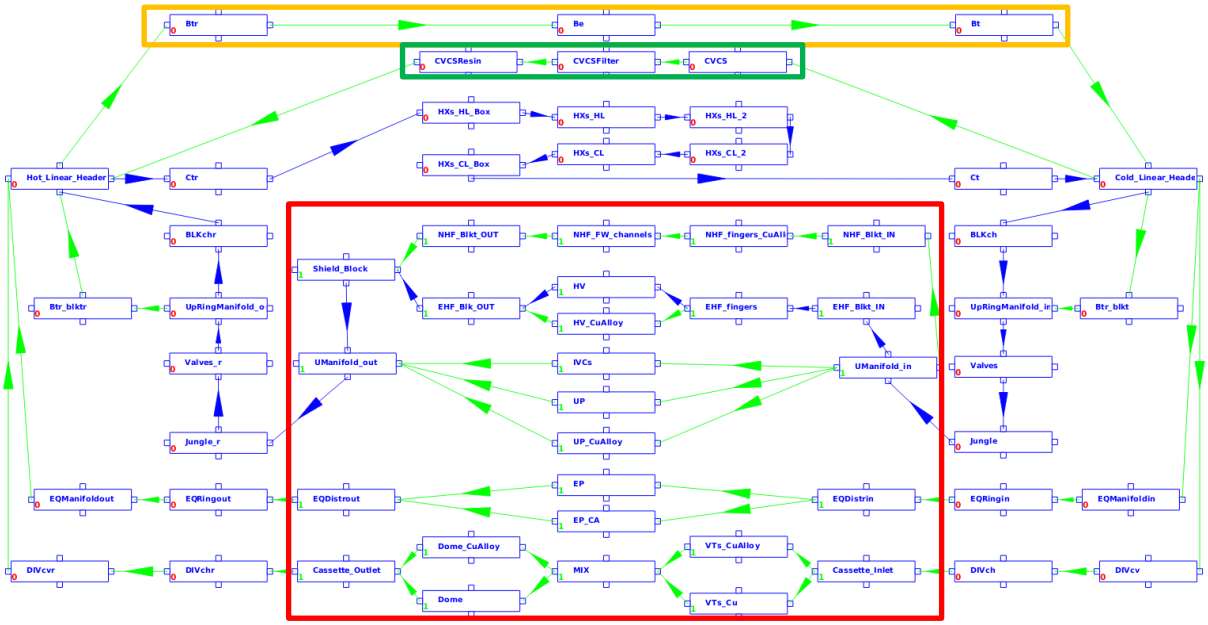

Figure 4: IBED PHTS OSCAR-Fusion input model: the orange rectangle frames the baking loop regions, the green rectangle frames the CVCS regions and the red rectangle frames the in-flux regions

The main improvements of this update consists in:
- The addition of equatorial ports clients and their piping distribution at equatorial level,
- The addition of the in-vessel coils and upper port clients at upper level,
- A better nodalization of the HXs volume and wet surface (from one region to 6)
- The introduction of the inlet and outlet isolation valves regions between the upper rings manifold and the jungle gyms,
- The checking and updating of the wet surfaces and hydraulic diameters on the basis of [27ZRW8] for all the out-of-flux regions of the IBED loop,
- Optimization of the FW-BLK regions with respect to [XQ7LQV] (smaller regions number).

- As a consequence of the above listed improvements, we obtained a general higher level of detail of the model compared to previous analyses [XNXW3N], [39CFJC].

3.4.2 IBED materials

The coolant circulating in the IBED loop interacts with different type of material; AISI316, AISI304, Oxygen free copper and copper alloy.
To better simulate the variety of materials used in different regions of the loop it was chosen to simulate 3 types of AISI 316, one type of copper alloy and one type of pure copper.
AISI304 (typically used for the out-of-flux piping) has not been simulated since its similar chemical composition to AISI316.
Materials composition and properties are summarised in the table below:

Table 5: Material composition and properties used in IBED model

Material name	AISI316_12 mic	AISI316_6 mic	AISI316_2 mic	AISI316_12 mic20	Cu alloy	Cu
Composition	Co 0.0005 Cr 0.175 Cu 0.003 Fe 0.648 Mn 0.018 Ni 0.123	Co 0.0005 Cr 0.175 Cu 0.003 Fe 0.648 Mn 0.018 Ni 0.123	Co 0.0005 Cr 0.175 Cu 0.003 Fe 0.648 Mn 0.018 Ni 0.123	Co 0.002 Cr 0.175 Cu 0.003 Fe 0.648 Mn 0.018 Ni 0.123	Co 0.0005 Cr 0.0075 Cu 0.99148 Fe 0.0002 Mn 2e-05 Ni 0.0003 Zr 0.0007[2]	Co 0.0005 Cr 0.0001 Cu 0.9991 Fe 0.0001 Mn 0.0001 Ni 0.0001
Roughness	12 µm	6 µm	2 µm	12 µm	1.3 µm	6.3 µm
Regions	Out-of-flux and in-flux regions	DIV stainless steel parts	HXs	Isolation Valves	In-flux regions	IVCs Divertor swirl tubes
References	[X83W55, [7VALZX]	[Appendix M]	[2F6J4N]	[89DGN3]	[Appendix M]	[WU8LSB]

3.5 Simplified Input and comparison with reference case

The i90 input is a *simplified* version of i9, i.e. it allows a significant reduction of the time required to complete a calculation and hence facilitate the comparison of the results of the parametric studies obtained varying both water chemistry (hydrogen content, Li injection) and operational set points (baking flow, CVCS flow).

The simplified i90 input has basically two main differences compared to the original i9:

- Reduced list of radionuclides, limited to the six gamma emitters: Co-58,Co-60, Cr-51, Cu-64, Fe-59, Mn-54
- No printing of the dwell time

The choices listed above were made to speed-up the calculations and reduce the size of the output files thus to facilitate the comparison between different runs; on the other hand, the accuracy of the results have been checked to ensure the coherency between the i9 and i90 in terms of data suitable for ORE studies.
To this purpose, hereafter the simplified case (i90) is compared to the reference one (i9) to check the consistency of the data and highlight the differences and their causes.

[2] Zirconium concentration is not simulated in OSCAR runs due to its negligible impact in terms of both activity and contribution to the ORE, as reported in [87D6BT]

3.5.1 Activity in the out-of-flux regions

Figure 5-7 show the results comparison in terms of overall activity for the i9 and i90 cases.

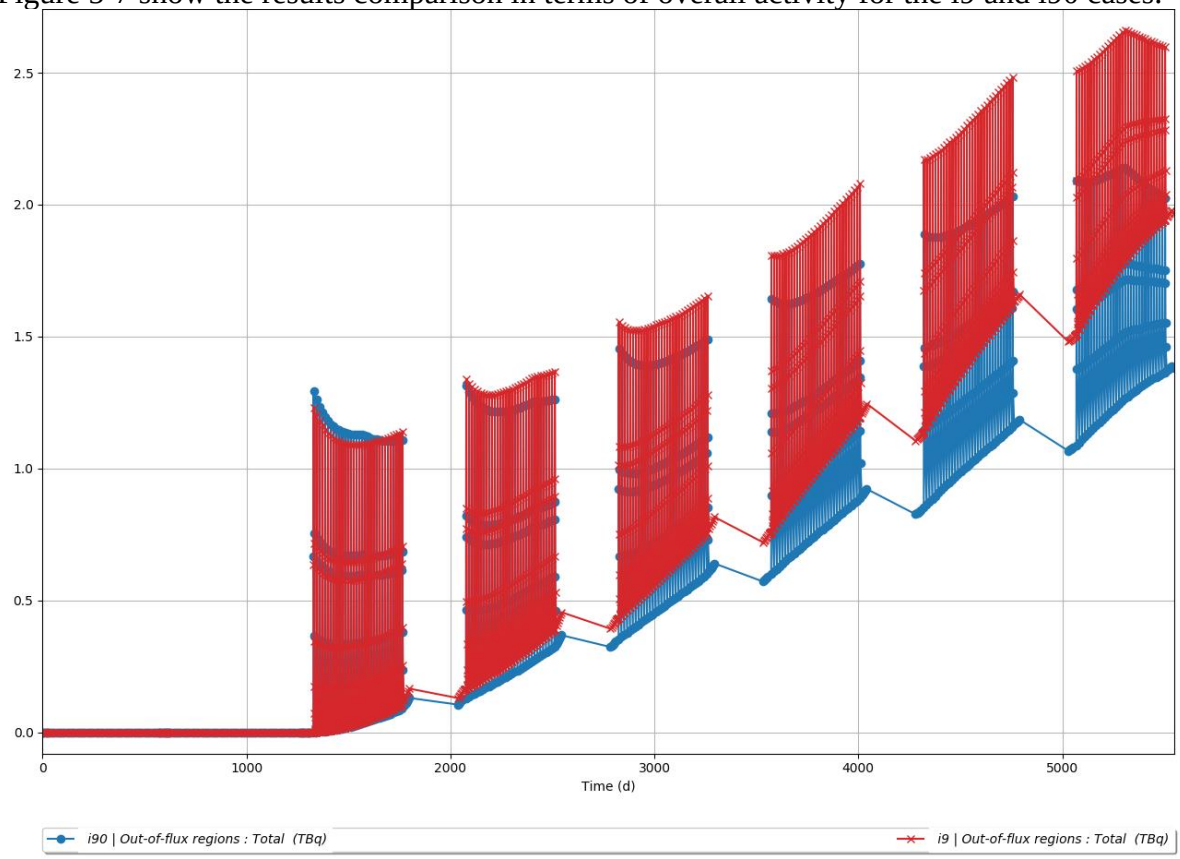

Figure 5 : Comparison of the overall activity (TBq) in the out-of-flux regions between the reference case (i9) and the simplified one (i90)

The results demonstrate a good agreement between the reference case and the simplified one: the shown delta (blue curve higher than the orange one) is due to the larger number of isotopes considered in the i9 case (mainly due to beta-emitter isotope Fe-55, hence not considered in the i90 case).

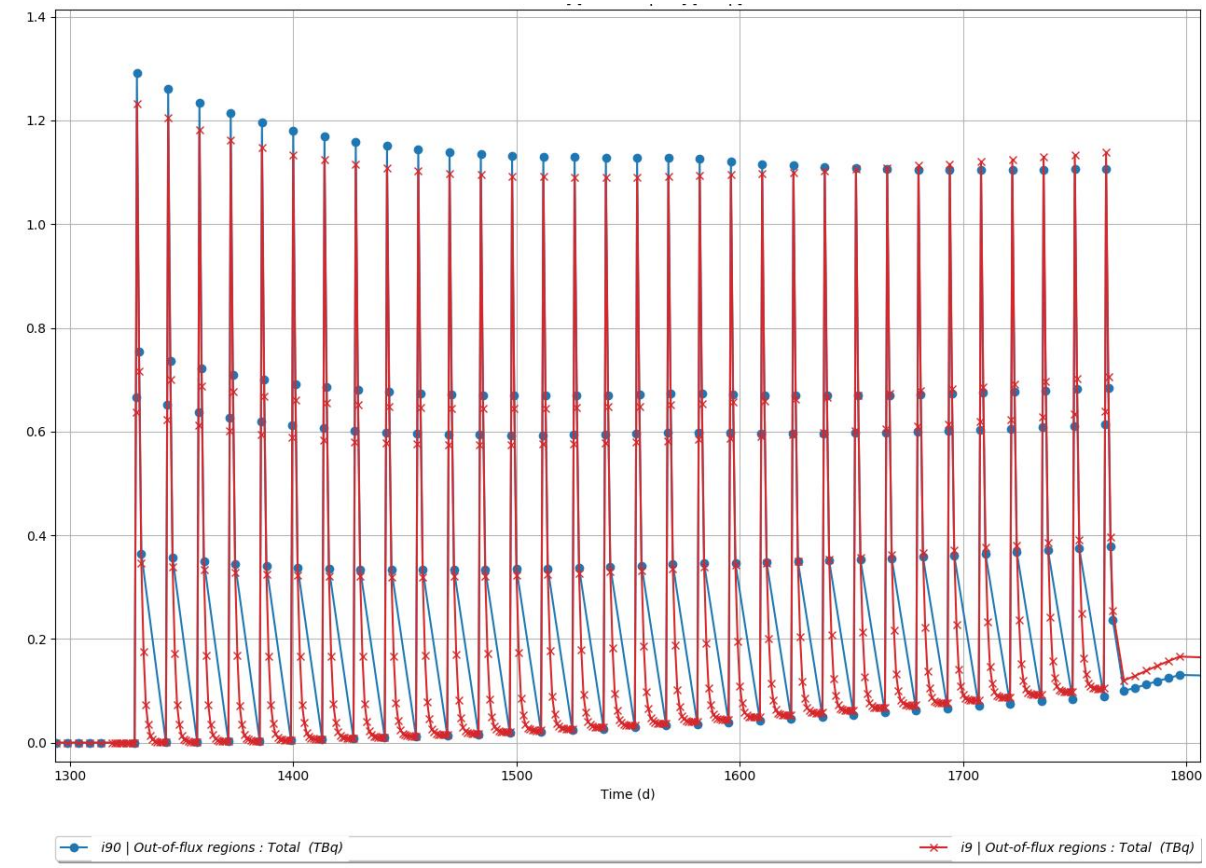

Figure 6: Detail of the first Fusion Plasma Operation (FPO1-3) – comparison of i9 and i90 Total Activity [TBq] in the Out-of-Flux regions

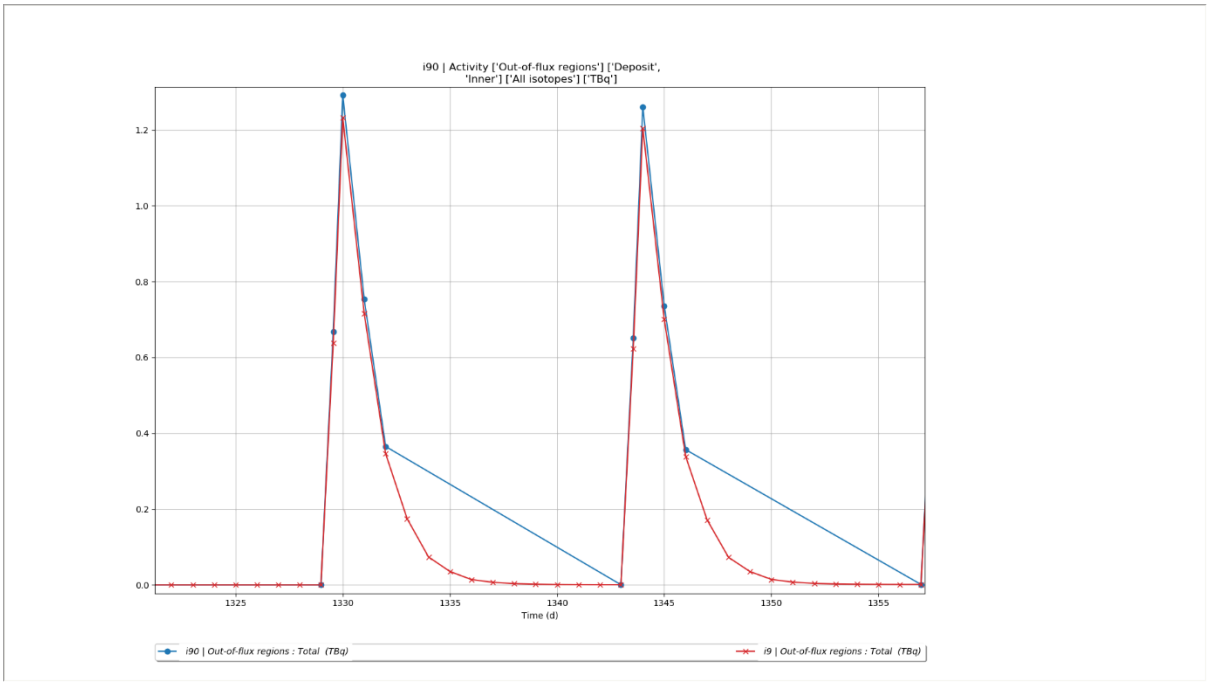

Figure 7 : Detail of the first two plasma sessions – comparison of i9 and i90 Total Activity [TBq] in the Out-of-Flux regions

The comparison of the surface activity (Figure 8 and 9) in the Jungle Gym return (i.e. the hot leg part of the loop immediately outside the bioshield and hence downstream the in-flux regions in the upper part of the tokamak) confirm the overall good agreement between i9 and i90; most

importantly for what concerns the ORE, Figure 9 shows a very good agreement for the cobalt element gamma-emitters (Co-58 and Co-60), with the simplified case showing slightly higher values.

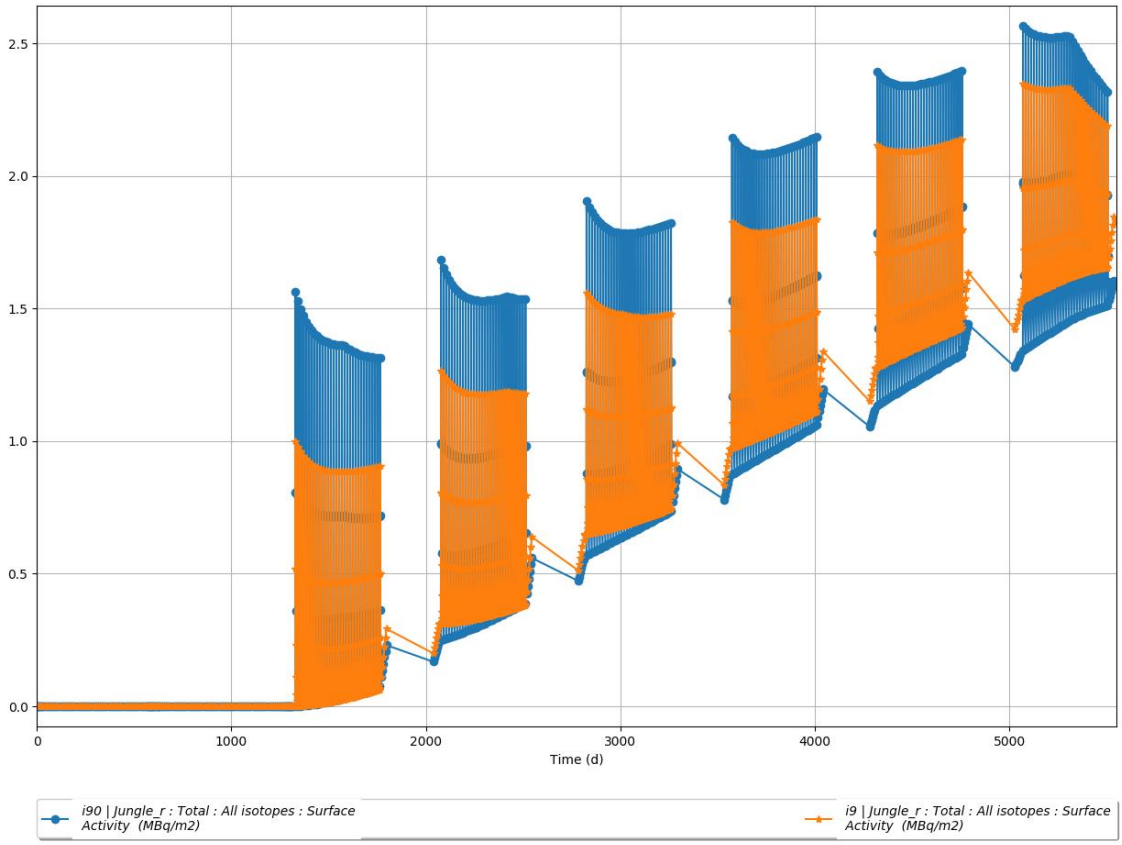

Figure 8 : Comparison of the surface activity (MBq/m²) in the Jungle Gym return region between the reference case (i9) and the simplified one (i90)

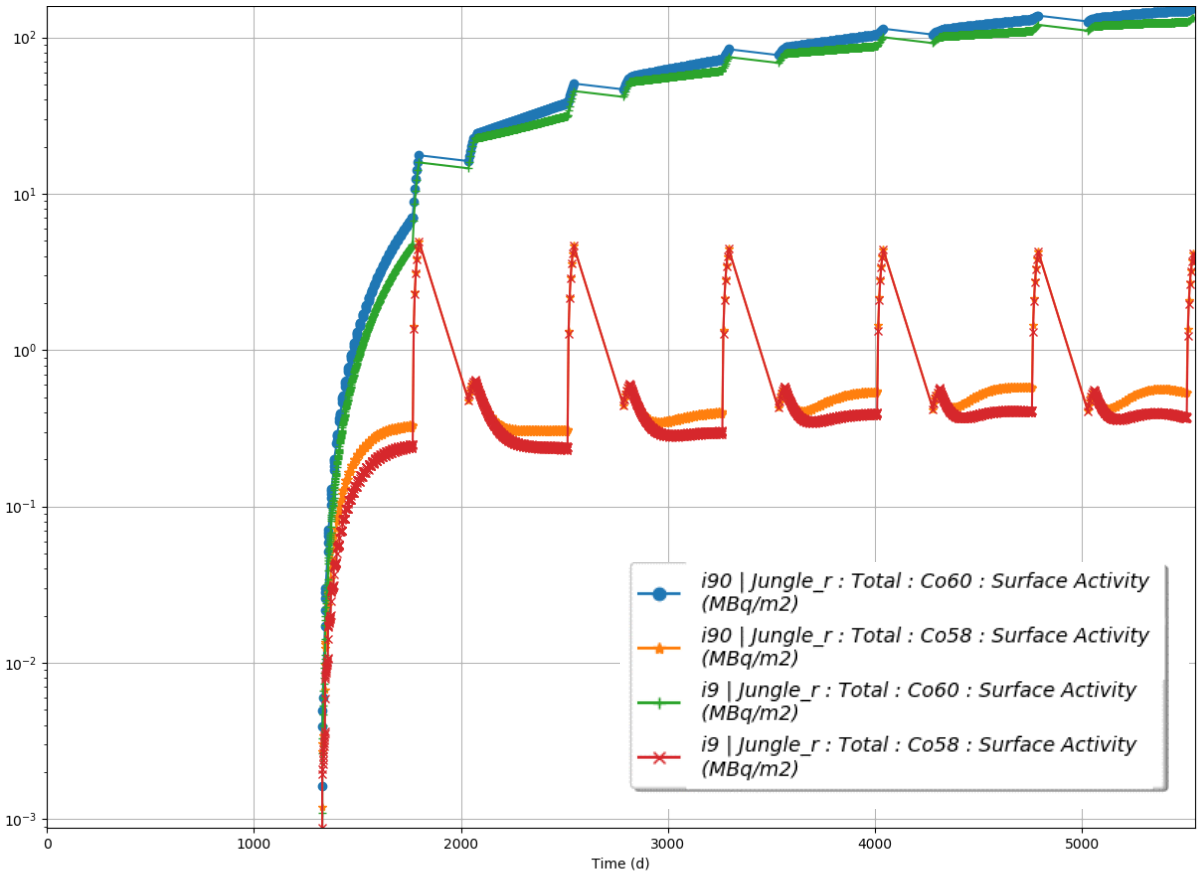

Figure 9 : Comparison of the Co-68 and Co-60 surface activity (MBq/m²) in the Jungle Gym return region between the reference case (i9) and the simplified one (i90)

3.5.2 Mass of Corrosion Products

Figure 10 below confirms the agreement between i9 and i90 results also in terms of mass of corrosion products (deposit + inner oxide) in both out-of-flux (blue and green) and in-flux regions (orange and red).

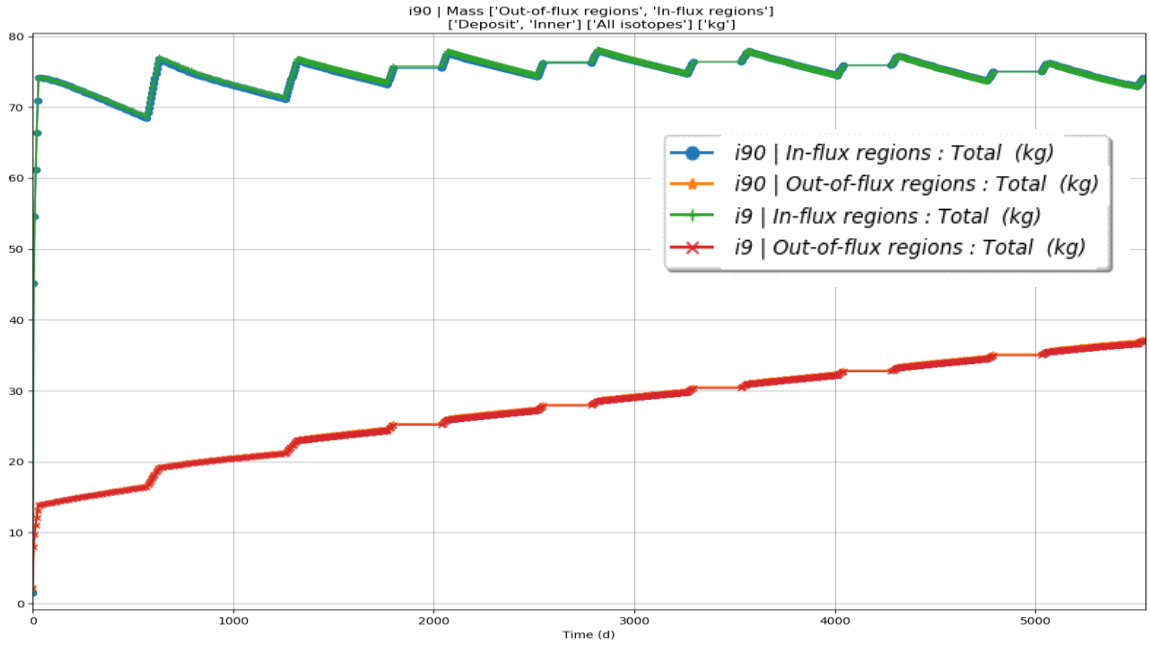

Figure 10 : Comparison of the mass (kg) of corrosion products in the Out-of-flux regions between the reference case (i9) and the simplified one (i90)

Corrosion products comprehend activated and non-activated ones; by way of example for the ratio between the two types, Figure 11 compares the out-of-flux mass for the deposits of the radioisotopes considered in the i90 cases element to the overall mass of deposit in the same regions.

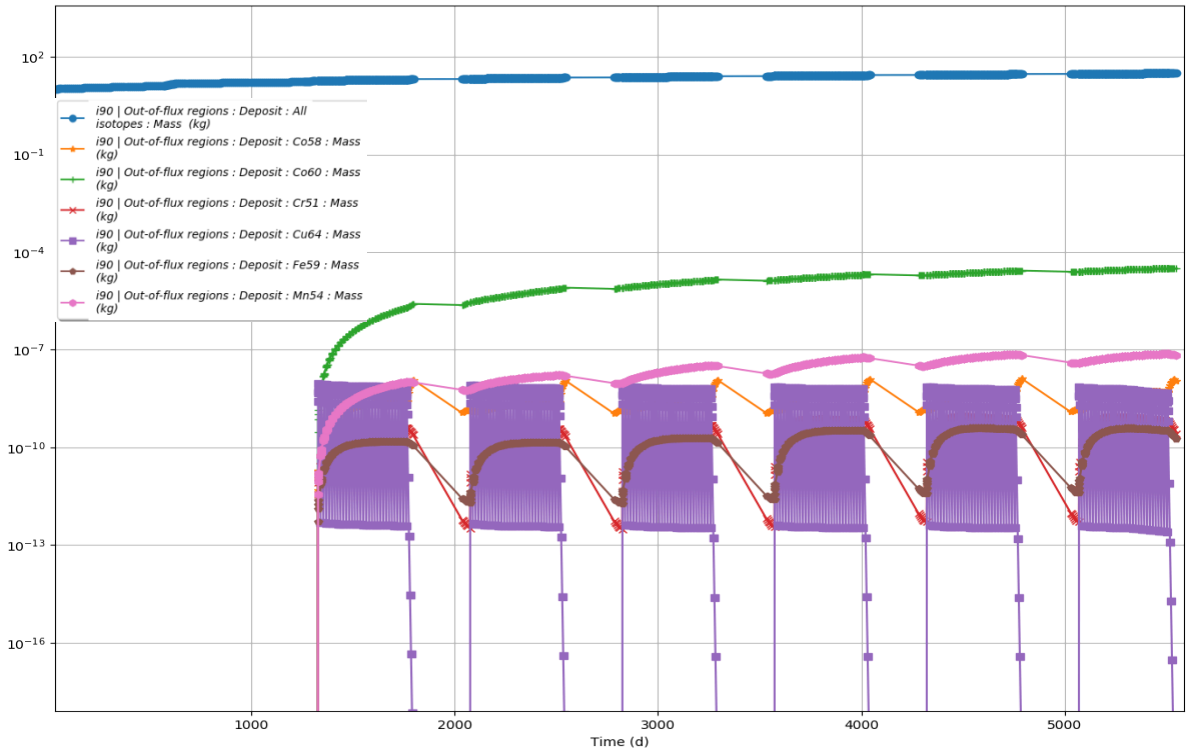

Figure 11 : Deposit mass comparison (kg) between the overall corrosion products and the radioisotopes ones in the out-of-flux regions

We can appreciate a delta of six order of magnitudes (factor 10^6) between the overall deposit mass and Co-60, i.e. the radioisotope with the largest mass among the ones (all gamma emitters) considered in this study.

Thus we can state that the overall mass of the corrosion products is primarily driven by the non-activated inventory; hence defining the total mass of corrosion products as "ACPs mass" it is misleading from a scientific point of view and simply wrong from an administrative one (i.e. for fusion reactors, safety objectives or limits on ACPs *should* refer to activity rather than mass).
For this reasons, ACPs limit shall be generically defined on the basis of overall and/or isotope specific activity.

Nevertheless, the overall CPs mass *is* actually a safety relevant information, for:

- some maintenance operations (e.g. frequency filter replacement and resins regeneration) are affected by the overall mass of corrosion products;
- monitoring the mass transport within the circuit before nuclear operation will give relevant information on the expected level of contamination during FPO (e.g. by applying the ratios shown above it is possible to estimate the contamination levels) and hence enabling test and optimization of established, bespoken good practices to reduce the contamination during the D-T operations.

3.5.3 Volume activity in CVCS piping

Figure 12 compares the coolant activity in the CVCS piping between i9 and i90: the results show a good agreement and the delta can be explained with the larger list of isotopes considered in the i9 case.

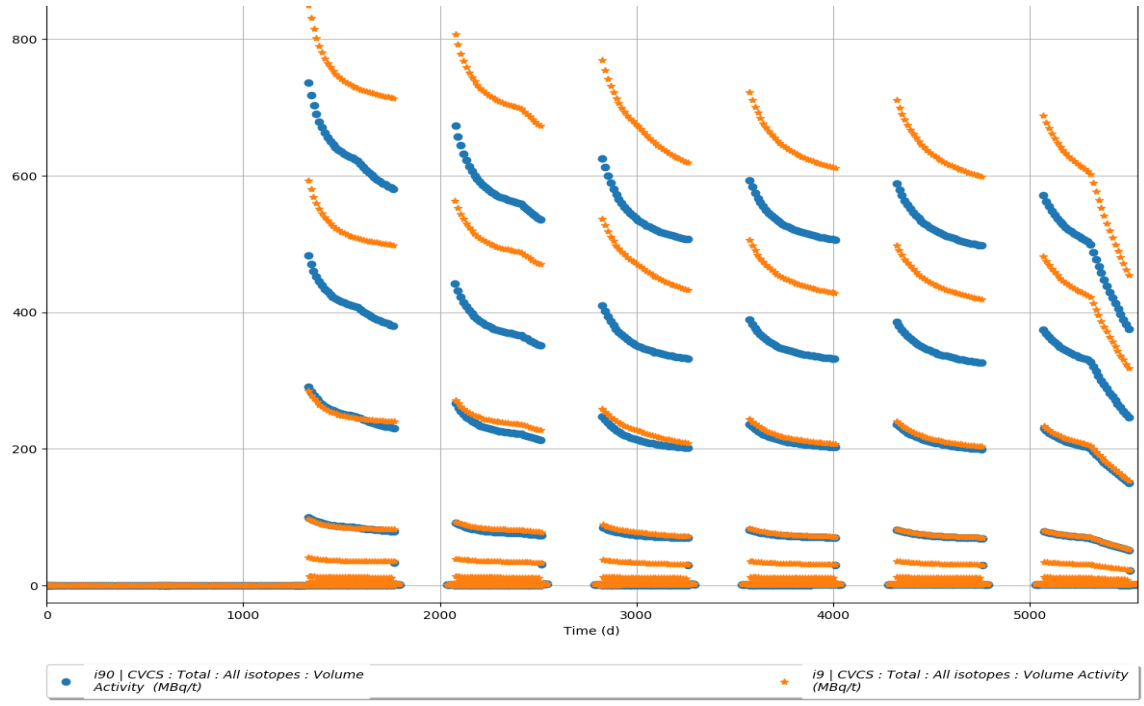

Figure 12 : Comparison of the activity in the coolant (MBq/t) in the CVCS piping between the reference case (i9) and the simplified one (i90)

3.5.4 *pH Control*

Figure 13 shows the pH variation during the whole duration of the calculation: in general, the pH value is around 7 during burn and baking operation and slightly above 8 during dwell, due to the lower temperature and same Li concentration than the burn phase.
pH variation is the same for both reference and simplified cases.

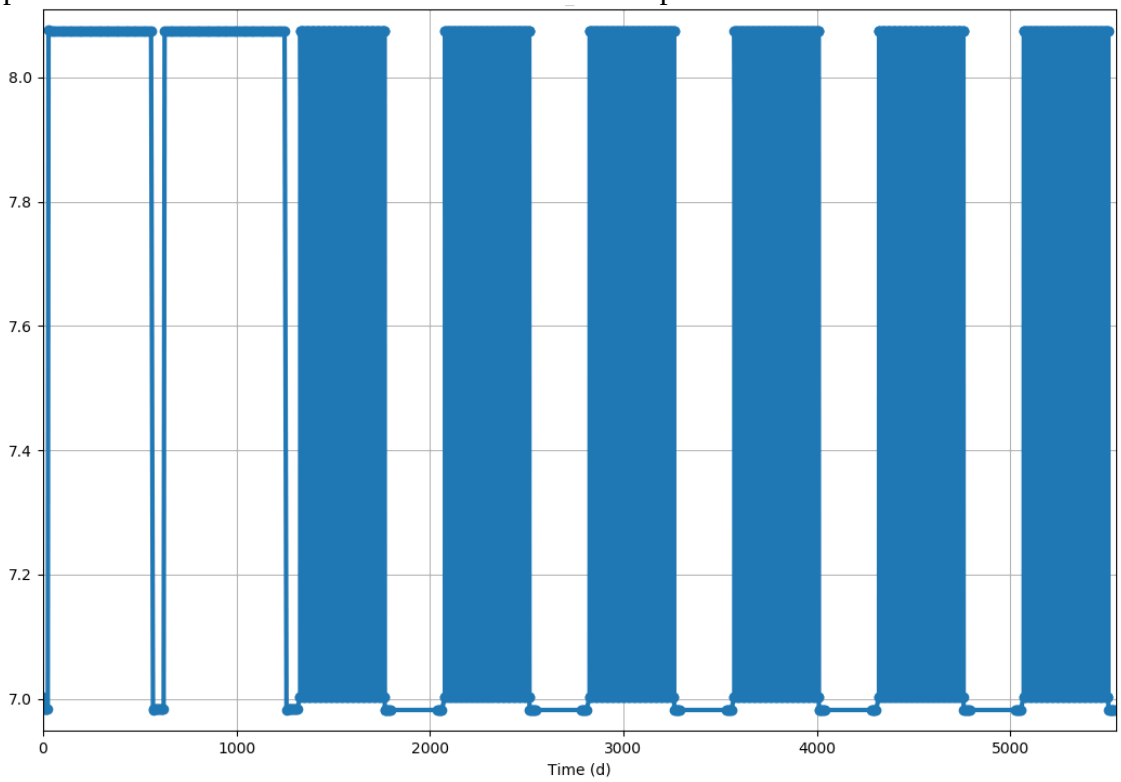

Figure 13 : pH behaviour for the i9/i90-cases

3.5.5 *Concentrations and Speciation*

To be completed/commented by Fred Dacquait

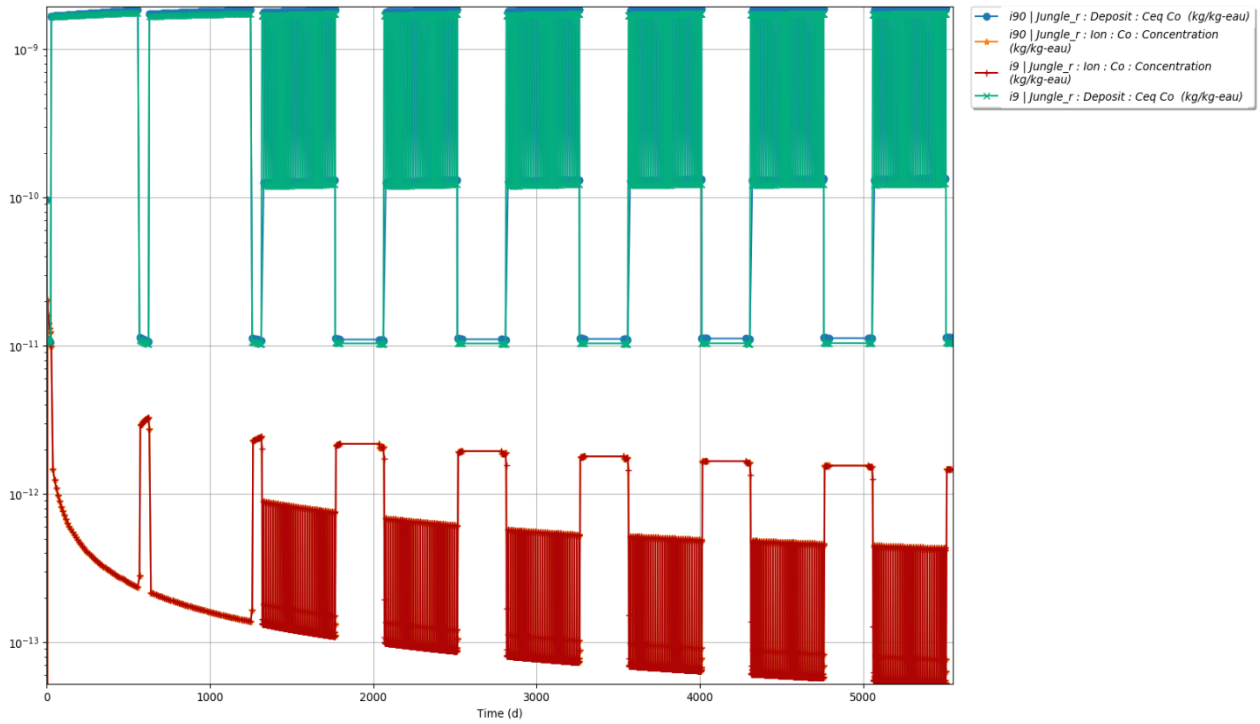

Figure 14 : Equilibrium and Ion concentration comparison between i9 and i90 cases

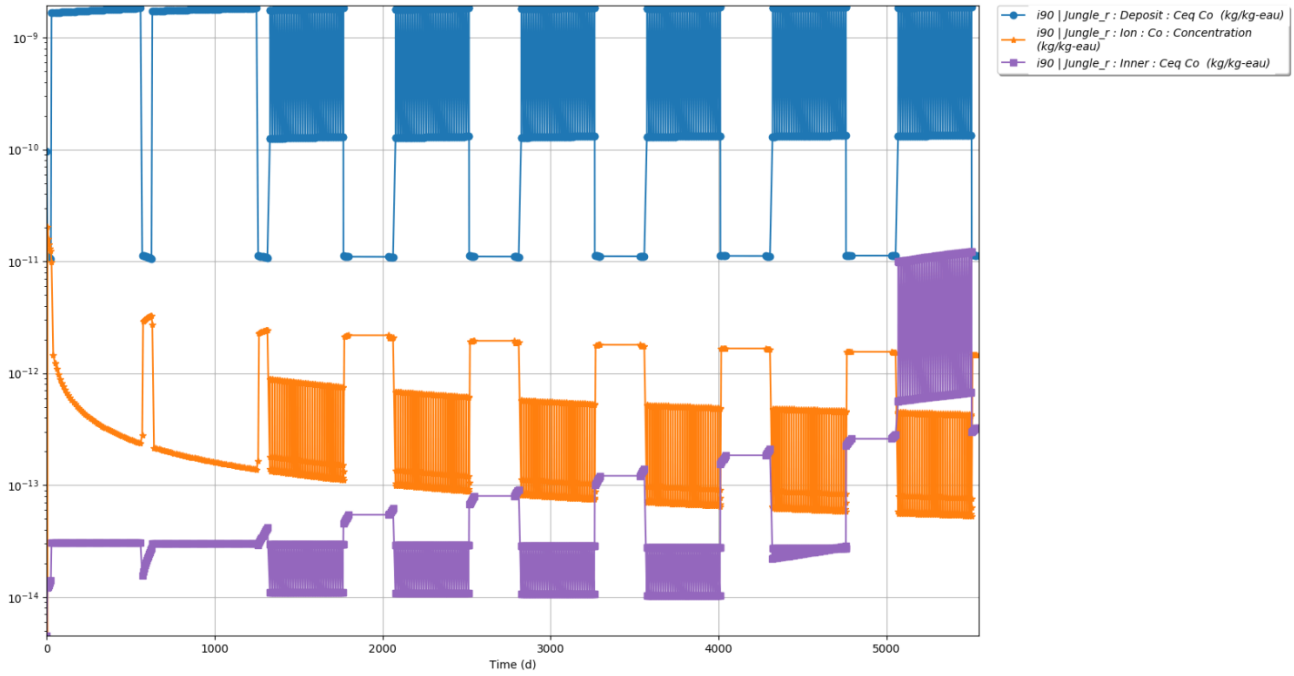

Figure 15: Ion, deposit and inner oxide concentrations for the i90-case

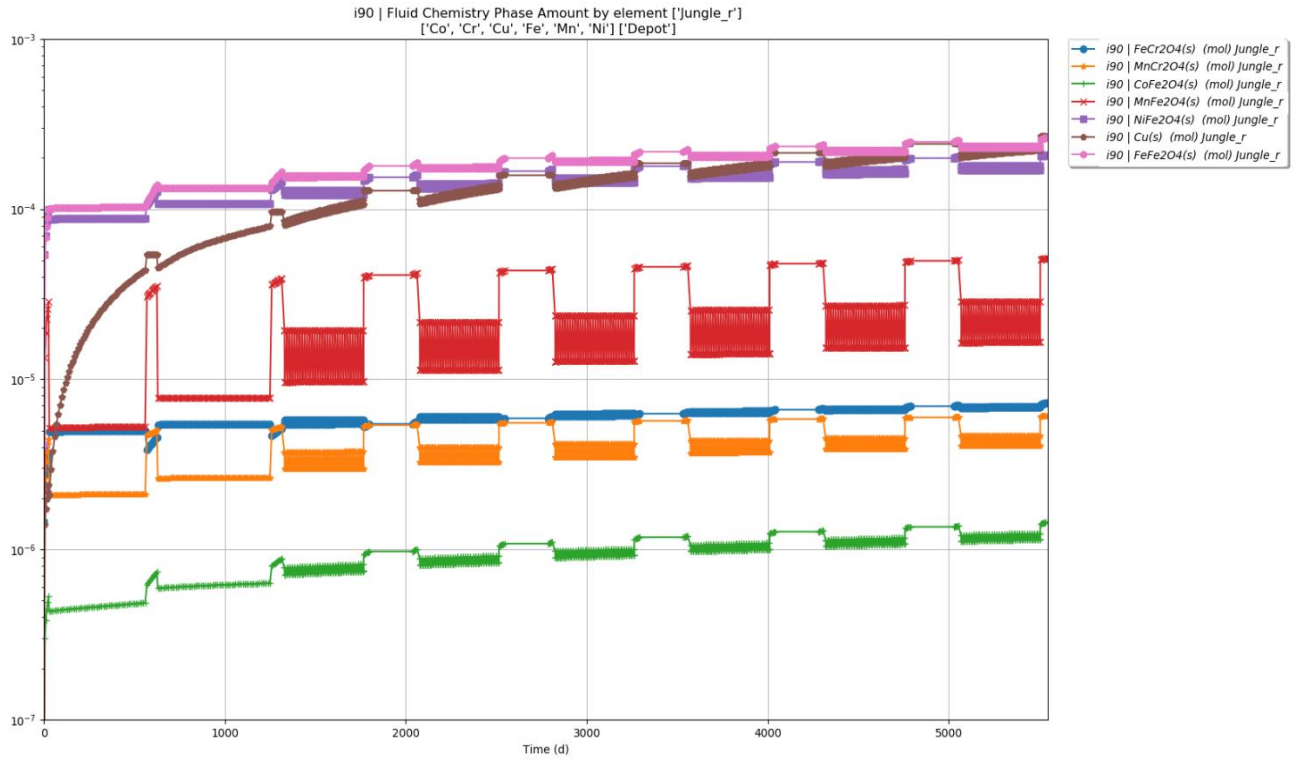

Figure 16: Speciation for the i90-case

3.5.6 Dose rates for the simplified case

Figure 17 shows the estimated contribution to the dose rate (at contact) for the Jungle_r region: the Contribution to the total is dominated by Co-60 after the end of the first plasma operation.

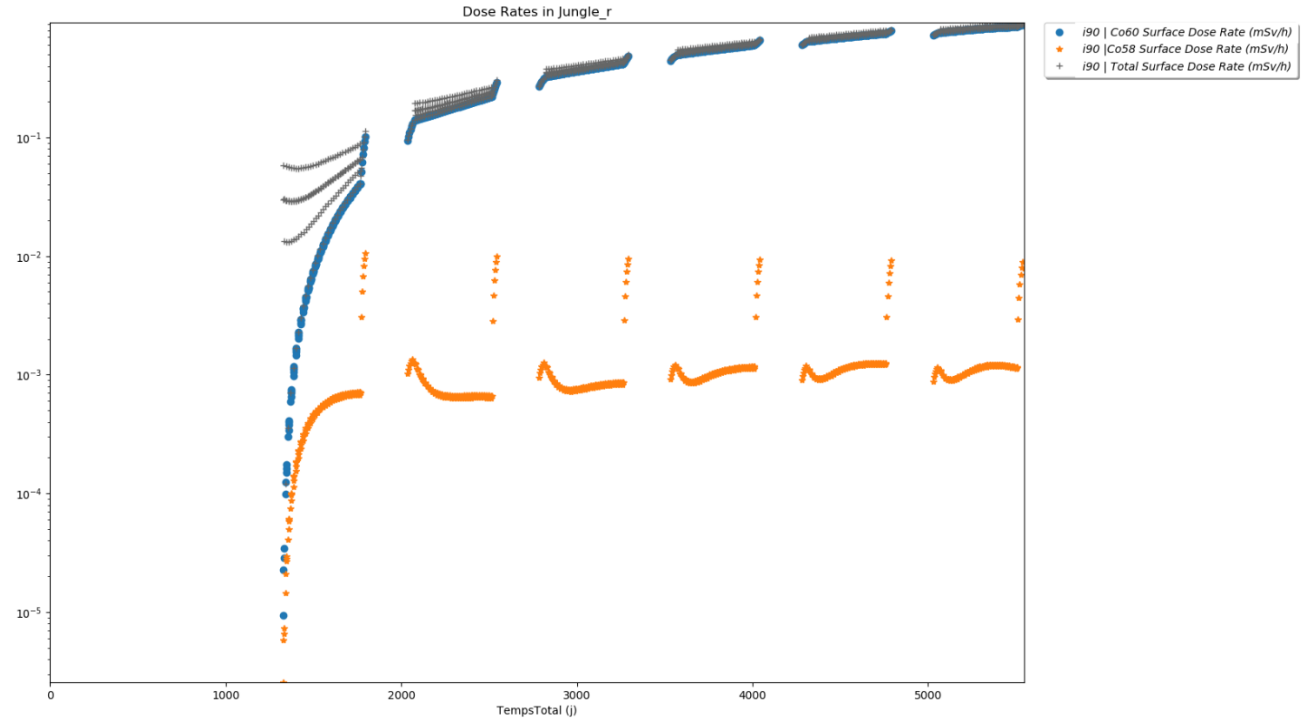

Figure 17 : Surface dose rate (mSv/h) – Co60, co58 and total dose rate in Jungle_r region

4 Coolant chemistry control for nuclear cooling systems

Basis on the operational experience from fission power plants [9FLNFB], the present section recall the rationale of the coolant chemistry control for pressurized nuclear cooling systems: the goal it to identify possible well-known chemistry control “strategies” also suitable for fusion devices.

4.1 Coolant chemistry control - generalities

Controlling the coolant chemistry in a nuclear reactor cooling loop is of utmost importance for several reasons:

1. Corrosion prevention: the primary objective of coolant chemistry control in a nuclear power plant is to prevent corrosion of reactor components, such as fuel cladding, pipes, and heat exchangers. Corrosion can degrade the structural integrity of these components, leading to leaks, equipment failure, and safety hazards. By maintaining appropriate coolant chemistry, i.e. by means of active analysis and control of the coolant, the reactor system can minimize corrosive conditions and protect critical components.
2. Radiological and contamination control: Controlling coolant chemistry helps mitigate the build-up and transport of radioactive and non-radioactive contaminants within the reactor cooling loop. These contaminants can include corrosion products, activated materials, fission products, and other impurities. Proper coolant chemistry management reduces the likelihood of contamination of the coolant, reactor surfaces, and equipment, thereby minimizing radiation fields and worker exposure to radioactive materials.
3. Heat transfer efficiency: The coolant chemistry can significantly impact heat transfer efficiency within the reactor system. Contaminants or deposits on heat transfer surfaces can impede heat transfer, leading to reduced cooling capacity and potentially compromising reactor safety. By controlling the coolant chemistry, the formation of deposits and scales can be minimized, ensuring efficient heat transfer and optimal reactor performance.
4. Neutron economy: The presence of certain impurities or chemical species in the coolant can affect the behaviour of neutrons within the reactor. Neutron-absorbing species, such as boron, can impact the reactivity and control of the nuclear chain reaction. Maintaining precise control over the coolant chemistry ensures the desired neutron economy and enables precise control of reactor power levels.
5. Material compatibility: The coolant chemistry should be carefully managed to ensure compatibility with reactor materials. Corrosive conditions or improper coolant chemistry can lead to material degradation, embrittlement, or stress corrosion cracking, compromising the structural integrity of reactor components. By controlling the coolant chemistry, the reactor system can minimize adverse interactions between the coolant and materials, enhancing the longevity and reliability of the reactor.

In summary, all the above listed points, with the exception of #4, apply also to a fusion reactor primary cooling system if water is chosen as coolant.

Therefore we can conclude that the effective control of coolant chemistry in a fusion reactor cooling loop is vital to prevent corrosion, control contamination, ensure efficient heat transfer and preserve the integrity of reactor components thus to play a crucial role in ensuring safe and reliable operation of the plant.

4.2 Hydrogen Concentration

Hydrogen injection can help mitigate radiolysis in a fission reactor cooling loop. Radiolysis is the process in which ionizing radiation, such as gamma rays or high-energy neutrons, break down the molecules in the coolant, leading to the formation of highly reactive chemical species. These reactive species can cause chemical reactions that result in the degradation of the coolant and the generation of additional contaminants.

Hydrogen injection is used as a method to control radiolysis by introducing molecular hydrogen (H2) into the coolant. Hydrogen is an effective scavenger of highly reactive species formed during radiolysis, such as free radicals. It acts as a sacrificial agent, reacting with the reactive species and stabilizing them, preventing further chemical reactions.

The injection of hydrogen into the coolant can help maintain the chemical stability of the coolant, reduce the formation of corrosive species, and minimize the degradation of coolant chemistry caused by radiolysis. This, in turn, helps prevent corrosion of reactor components, reduces the risk of coolant contamination, and preserves the overall integrity of the cooling loop.

It's important to note that the amount and method of hydrogen injection need to be carefully controlled to achieve the desired benefits without introducing any adverse effects. The concentration of hydrogen, the injection location, and the overall reactor design and operational considerations play a role in determining the effectiveness of hydrogen injection for mitigating radiolysis.

Hydrogen concentration for the IBED PHTS is set in a range of 10-60 ppm in [2823A2]; in both i9 and i90 cases the H2 set-point is 25 ppm.

4.3 Control of pH

4.3.1 Lithium hydroxide

Lithium hydroxide (LiOH) or Potassium is sometimes used in western fission reactors as a chemical agent for controlling the acidity (pH) of the reactor's coolant water. The rationale of injecting lithium into the coolant is explained in the following points:

1. pH control: Maintaining the proper pH level in the reactor's coolant water is crucial for several reasons. Firstly, it helps prevent corrosion of the reactor's structural materials, including the fuel rods and coolant pipes. Secondly, it helps maintain the effectiveness of the reactor's neutron-absorbing materials, such as boron, which are added to the coolant to control the reactor's power output. By injecting LiOH into the water, the alkalinity of the coolant can be increased, thus preventing excessive acidity and mitigating the risk of corrosion.
2. Chemical compatibility: Lithium hydroxide is chosen for pH control in nuclear reactors due to its favourable chemical compatibility with the reactor system. It has low reactivity with the structural materials and other components of the reactor, ensuring that it does not introduce any adverse effects or unwanted reactions.
3. Safety considerations: LiOH is preferred over alternative chemicals for pH control due to its relatively low toxicity and low radiotoxicity. It is considered a safer choice in

terms of handling, disposal, and potential environmental impact compared to some other chemicals.

The use of LiOH or any other pH control agent depends on the specific reactor design and operational requirements. Different types of reactors may employ different methods for pH control, and not all reactors use LiOH (e.g. VVER, see next section).

4.3.2 Potassium hydroxide

In VVER reactors, KOH is added to the coolant water as part of the water chemistry program for several purposes:

1. pH control: KOH is used to adjust and maintain the proper pH level of the coolant water. Controlling the pH is essential to prevent corrosion of reactor components and maintain their integrity.
2. Suppression of radiation field build-up: By maintaining appropriate pH levels with the help of KOH, the accumulation of radioactive corrosion products can be minimized. This helps reduce the radiation fields within the reactor system and improves the overall radiation protection.
3. Water chemistry balance: The addition of KOH in VVER reactors helps maintain the desired water chemistry balance by controlling the concentrations of various chemical species, such as dissolved oxygen and hydrogen. This ensures optimal reactor operation and reduces the potential for corrosion or other undesirable effects.

It's important to note that the specific water chemistry program and the use of KOH may vary between different VVER reactors and operational requirements.

4.4 ITER

The current strategy for ITER primary cooling water system is summarized in the table below:

Table 6 - Cooling Water Chemistry Specification for Plasma Operation [2823A2]

	Mode	Plasma	Baking		
Parameter	Unit	IBED PHTS	IBED PHTS	Current consideration	Comment from the authors of this report
Conductivity @25°C	µS/cm	<= 0.2	*		Not possible to control the primary coolant conductivity during operation – maybe this applies to the feed water – anyway by injecting ammonia this conductivity set point cannot be achieved – Conductivity monitoring
pH @25 °C	-	7.0 - 9.0	*		
Sodium	ppb	<= 5	<= 5	No reason to increase/decrease during Baking	
Chloride	ppb	<= 5	<= 5	No reason to increase/decrease during Baking	
Hydrogen**	ppb	<= 80	-	No injection expected during baking (no radiolysis)	
Catalyzed Hydrazine***	ppb	<= 30	-	Injected for only initial filling	
Ammonia***	ppb	<= 1,000	-	No injection expected during baking, but could be injected to control pH	Ammonia to control the pH in a circuit with Cu alloy as structural material might lead to high corrosion rates: this choice shall be justified against experimental data proving that ammonia doesn't enhance the Cu alloy corrosion (and corrosion/erosion) phenomena However, ammonia will be generated by combination of water radiolysis and hydrogen injection (like in BWR)?

					In the reducing condition, N16 exist as NH_3 $n+O_{16}=N_{16}+p+\gamma$ - Not clear if this quantity is limited to the injection or if it also considered the contribution of radiolysis
Oxygen	ppb	<= 10	<= 10	No reason to increase/decrease during Baking	
ORP@25 °C	mV	(-400) - (-100)	*		
Iron****	ppb	<= 10	*		Not controllable unless for feed water: once injected in the circuit there are no means to control the metal concentration; moreover the metal media shall be specified (**ions, particles or total?**) What is the technical basis for these values (see below)
Copper****	ppb	<= 10 (to be 13 ppb due to PCR1054)	*		Same as above

* The water chemistry specifications given in this table are valid for plasma operation only. Specifications for baking operation will be established and refined on the basis of operational experience.
** The decision on the use of hydrogen for chemistry/radiolysis control is pending.
*** The use of controlling chemicals (ammonia, catalyzed hydrazine) is based on chemistry control needs.
**** The iron and copper limits are tentative and subject to change.

5 Parametric studies

Our goal is to investigate contamination reductions measures: to this purpose we considered different parameters.:

- H2 concentration
- pH control & Baking operation
- CVCS flow rate
- Pipe roughness

The comparison of the results focuses on:

- Overall out-of-flux activity
- Jungle and Jungle-r total surface activity for Co-60

5.1 Hydrogen Concentration

The typical H2 concentration used in i9 and i90 calculations is of 25 ml/kg of water (250 ppb). Four alternative H2 concentrations have been simulated to investigate the impact on the ACPs inventory: 5, 15, 40 and 60 ml/kgw (millilitre per kilogram of water), named respectively H5, H15, H40 and H60.
In the following, the figures showing the comparison between these 4 cases.

5.1.1 Overall Out-of-flux activity

Figure 18 shows the results in terms of overall activity (deposit + inner oxide) in the out-flux regions for the four cases:

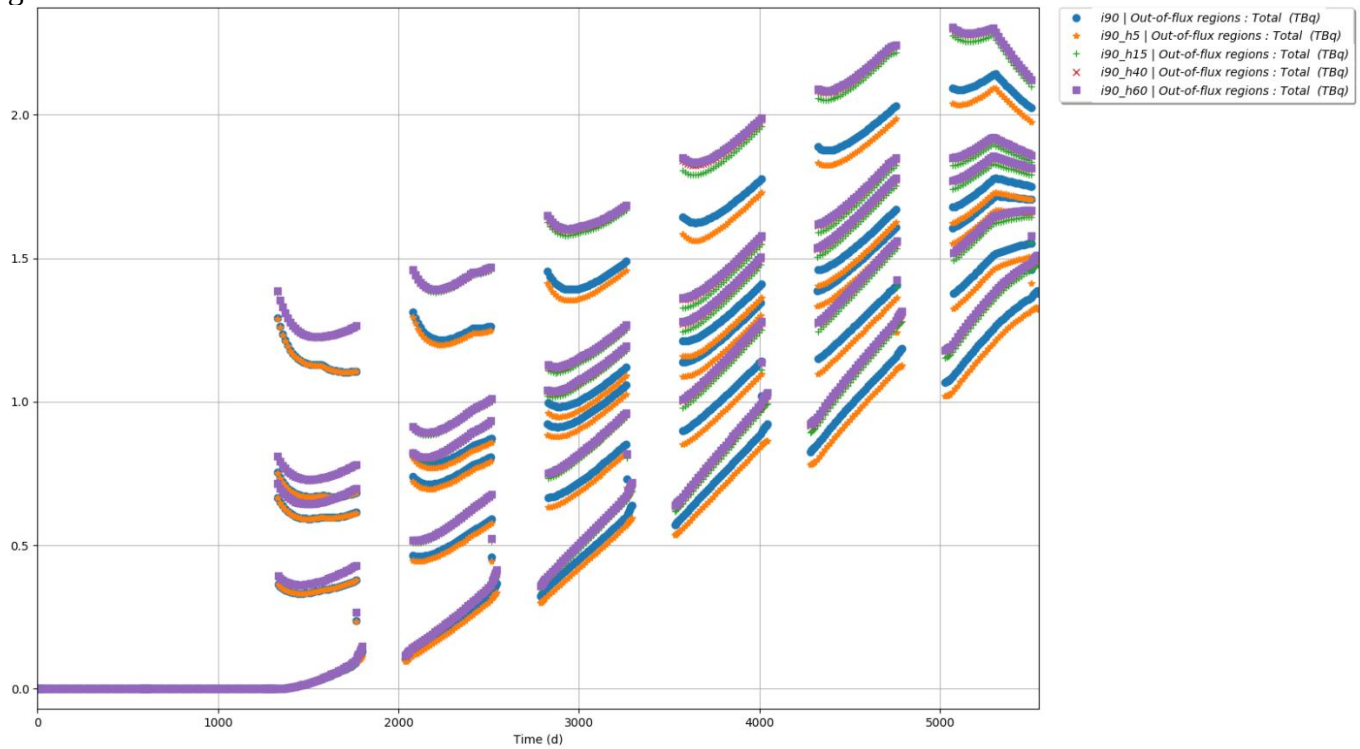

Figure 18 : Out-of-flux activity (TBq) comparison varying the H2 concentration

It is possible to observe that the overall effect of the variation of H2 concentration in the range 5-50 ml/kgw has a very limited impact on the results; the case at 5 ml/kgw is the one with the

lowest activity value, therefore we can preliminary conclude that ideal H2 concentration shall be kept as low as possible in the IBED loop.
The simplified case (H2 concentration at 25 ml/kgw) shows overall activity values higher than i90_h5 case but lower than all the other tested H2 concentrations: this “local minimum” can be explained by a numerical fluctuation of the results as a consequence of the automatic calculation of the relaxation length in the circuit by the code.
In general, the results of overall activity as a H2 concentration suggest that the lower the H2 content the better; however, the possible radiolysis occurring in the in-flux regions interacting with neutrons will generate oxygen molecules/atoms and hence it will introduce the potential for local oxidising conditions, definitely not favourable to limit the corrosion of the base metal. Therefore, further dedicated studies on the optimal H2 content for the IBED loop, ideally with the support of experimental tests, are required.

5.2 pH control

As previously done in [87D6BT], the i90 case simulates lithium injection during all the operational modes to keep coolant pH above 7 and hence avoid potential high-corrosive environment for the base metals, in particular for the Cu alloy.
To estimate the effect of pH variation on the overall contamination of the out-of-flux regions, we modified the simplified input for parametric studies considering:

- Nobake - No baking operation between plasma campaigns
- lowbake – i.e. flow rate reduction of a factor 10 during baking
- NL - No lithium injection
- LB - Lithium injection for pH control only during baking operations
- LPO - Lithium injection for pH control only during burn and dwell operations

The results in terms of activity in the out-of-flux regions are shown together with the i90 ones for comparison in Figure 19.

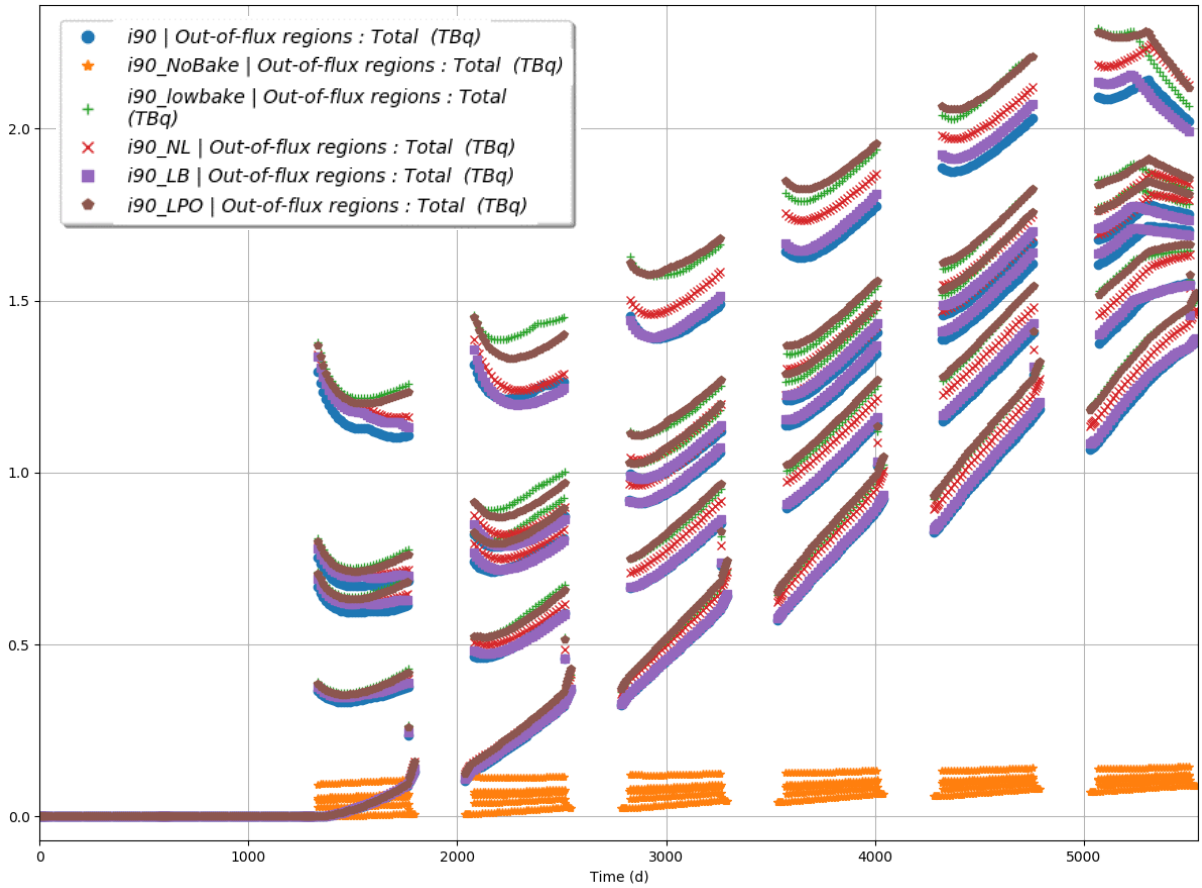

Figure 19 : comparison of i90 with no-lithium case

The comparison of the results shows that there is moderate difference in terms of overall activity between all the cases with the remarkable exception of the NoBake case: this is also due to the reduced list of isotopes considered for this studies (e.g. Fe55 is excluded from the calculation and hence the effect of Li injection is limited to the gamma emitters).
According to these results, to limit the spread of contamination, it would be hence favourable to:

- Avoid water baking as long as possible
- Keep the baking flow rate at the nominal value
- Avoid lithium injection during plasma operation (burn and dwell)

Pros and cons of such a pH control strategy should be carefully analysed and supported by future experimental evidence.

5.3 CVCS flow rate

The flow rate CVCS is set in [2823A2], nevertheless we investigated the impact in terms of circuit contamination of varying such a flow rate.
The i90_CV10 case simulates an increased flow rate for the CVCS up to 10% of the nominal flow for the entire loop during baking.
Figures 20 and 21 below show that such a CVCS flow rate increase would have a beneficial effect in terms of reduction of the overall and Co-60 surface activities.

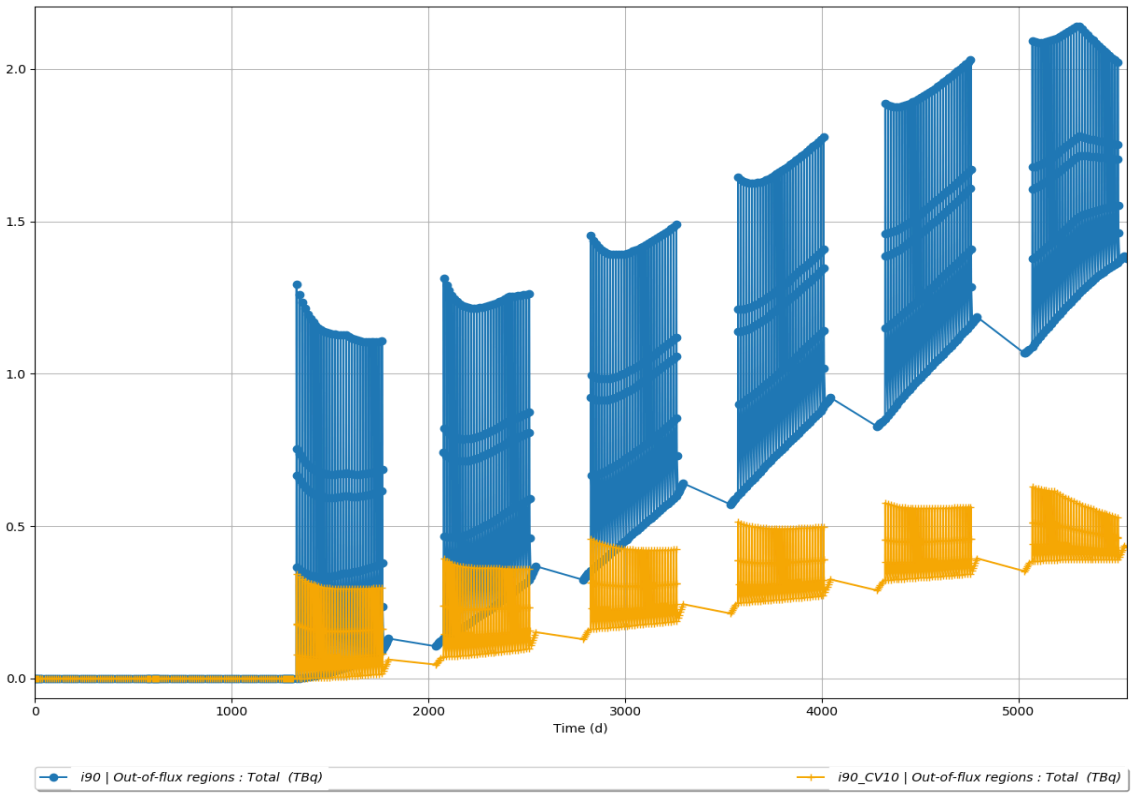

Figure 20 : Comparison of the overall activity in in the out-of-flux regions between reference scenario and the one with increased CVCS flow rate

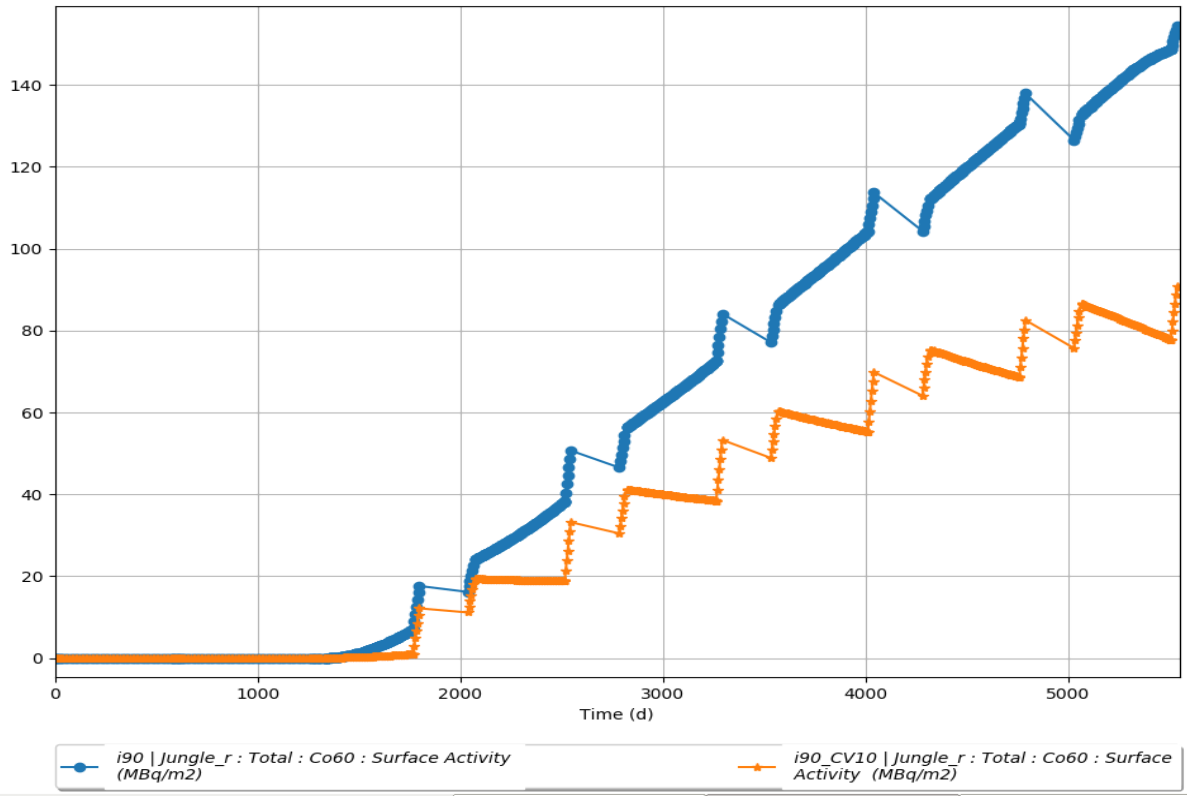

Figure 21 : Comparison of the Co-60 surface activity in in the Jungle_r region between reference scenario and the one with increased CVCS flow rate

5.4 Pipe roughness

To evaluate the impact of the piping roughness on the activity of the regions outside of the flux, a study case was launched using a reduced roughness, 2 microns, for the Jungle Gym piping (inlet and outlet) to be compared to the reference case, which considers the "standard" roughness of 12 microns (requirement for TCWS piping) [2823A2]. The Figure 22 hereafter highlights a 50% reduction in the overall surface activity due to Co-60 for the Jungle Gym return piping for the 2 microns case. Figure 23 shows that such reduction in activity finds its explanation in the lower deposit thickness on both hot and cold legs of the Jungle Gym for the reduced roughness case.

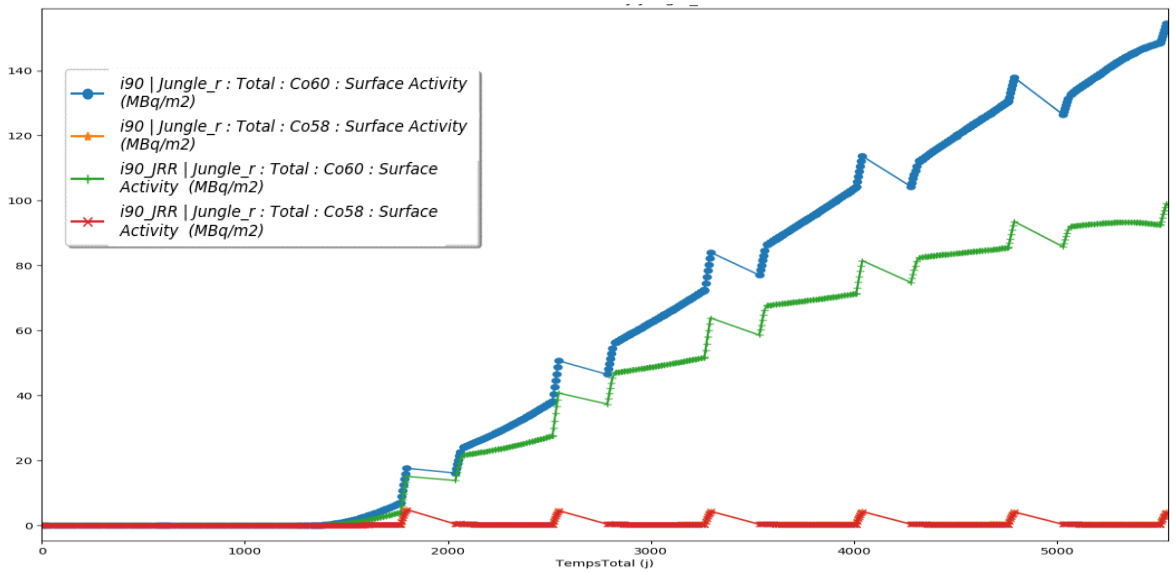

Figure 22 : comparison of the Co-60 and Co-58 Surface Activity (deposit plus inner oxide) in the Jungle Gym return piping for the reference case and the reduced roughness one

Figure 23 : Deposit thickness for Jungle Gym distributions – comparison between reference and reduced roughness

Summary, Conclusions and recommendations

This report gives an overview of the parametric studies conducted to investigate the impact on the ACPs source term of both coolant chemistry and operational strategies.
The reference model for ACPs assessment has been simplified to enable quicker and lighter calculations and comparison of the results.
The parametric studies focused on the coolant chemistry control (H2 concentration, pH, operational strategies (baking, CVCS flow rate) and finally design choices (pipe roughness in ORE high-impacting areas).
Results have been compared to the simplified case in terms of overall activity in the out-of-flux regions and total surface activity due to Co-60 in the Jungle Gym return piping.

Such a comparison highlights:

- Positive impact of low H2 content on the overall spread of the contamination
- Additional work required to assess the feasibility to keep H2 concentration at 5 ml/kgw during plasma operation and its effectiveness in preventing oxidising atmosphere formation in the regions exposed to potential coolant radiolysis (i.e. in-flux regions)
- Positive impact of avoiding baking operation to minimize the out-of-flux regions contamination – such a "simple" solution might be demonstrated ensuring that realistic alternative strategies for the cleaning (i.e. tritium and impurities removal) of the in-vessel components can be implemented in the operational strategies without compromise the scientific programme nor the integrity of the systems
- Positive impact of CVCS flow rate increase during baking operation
- Positive impact of roughness reduction in specific regions to limit the contamination in such piping/equipment

Next, further ACPs studies shall be performed consideringthe following reccomendation:

- Update of the corrosion rates of AISI, Cu and Cu alloy based on experiments with the expected water chemistry such as ammonia, LiOH and etc.
- LiOH is proven chemical in the PWRs, no adverse effect on SS and Ni alloys; however, no data for Cu and Cu alloys are available: therefore it is recommended to have a test using Cu and Cu alloys with LiOH (For example, comparison tests using LiOH and ammonia to justify usage of LiOH instead of ammonia)
- Verification of the negligible impact of considering Zr in the CuCrZr in terms of corrosion phenomena and contribution to the ORE

Finally, we recommend to the operators/system owners to:

- Identify optimal coolant chemistry condition for all operating conditions, including:
    - H2 concentration
    - pH controls
    - O2 control
    - Contaminants control following EPRI
- Demonstrate the feasibility of using ammonia for a copper-based system
- Implement roughness reduction in the regions of the circuits were maintenance/inspection activities contributes significantly to the overall ORE
- Study impact of the CVCS flow rate increase
- Study alternatives to the water baking or if not possible in any case,
- Limit baking frequency and duration

Appendix G – IBED Cooling loop OSCAR Geometry input

ID	Region Name	Material	Roughness [µm]	Wet surface [m²]	Dh [m]	G factor	Fluid velocity [m/s]	NZ	Ref.
1	BLKch	AISI316	12	54	0.456	1	3.4	0	[XQ7LQV][RWBRH3]
2	BLKchr	AISI316	12	62	0.456	1	3.4	0	[XQ7LQV][RWBRH3]
3	Be	AISI316	12	72	0.231	1	0	0	[XQ7LQV][RWBRH3]
4	Bt	AISI316	12	28	0.224	1	0	0	[XQ7LQV][RWBRH3]
5	Btr	AISI316	12	44	0.266	1	0	0	[XQ7LQV][RWBRH3]
6	CVCS	AISI316	12	18.84	0.1	1	2.1	0	[XQ7LQV][RWBRH3]
7	Ct	AISI316	12	524	0.445	1	4	0	[XQ7LQV][RWBRH3]
8	Ctr	AISI316	12	524	0.445	1	4	0	[XQ7LQV][RWBRH3]
9	DIVch	AISI316	12	1154	0.164	1	2.3	0	[XQ7LQV][RWBRH3]
10	DIVchr	AISI316	12	921	0.164	1	2.3	0	[XQ7LQV][RWBRH3]
11	DIVcv	AISI316	12	48	0.409	0	6.7	0	[XQ7LQV][RWBRH3]
12	DIVcvr	AISI316	12	79	0.409	0	6.7	0	[XQ7LQV][RWBRH3]
13	Jungle	AISI316	12	205	0.206	0	3	0	[XQ7LQV][RWBRH3]
14	Jungle_r	AISI316	12	123	0.248	0	3.8	0	[XQ7LQV][RWBRH3]
15	UpRingManifold_in	AISI316	12	291	0.31	0	7.3	0	[XQ7LQV][RWBRH3]
16	NHF_Blkt_IN	AISI316	6.3	133	0.095	1	1.3	1	[XQ7LQV][RWBRH3]
17	EHF_Blkt_IN	AISI316	6.3	161	0.032	1	4.1	1	[XQ7LQV][RWBRH3]
18	NHF_channels	AISI316	6.3	418	0.022	0	1.1	1	[XQ7LQV][RWBRH3]
19	EHF_fingers	AISI316	6.3	53.4	0.012	1	7.4	1	[XQ7LQV][RWBRH3]
20	NHF_Blkt_OUT	AISI316	6.3	224	0.073	1	1.7	0	[XQ7LQV][RWBRH3]
21	HV	AISI316	6.3	828	0.009	1	1.9	0	[XQ7LQV][RWBRH3]
22	HV_CuAlloy	CuCrZr	1.3	644	0.009	1	3.8	0	[XQ7LQV][RWBRH3]
23	IVCs	Cu	6.3	40	0.03	1	2	0	[89DGN3]
24	EHF_Blk_OUT	AISI316	6.3	207	0.026	1	3.8	0	[XQ7LQV][RWBRH3]
25	Shield_Block	AISI316	6.3	2203	0.021	1	1	0	[XQ7LQV][RWBRH3]
26	UP	AISI316	6.3	244	0.063	1	2	0	[89DGN3]
27	UpRingManifold_out	AISI316	12	317	0.309	0	7	0	[XQ7LQV][RWBRH3]
28	Cassette_Inlet	AISI316	6.3	392	0.086	1	2.05	0	[XQ7LQV][RWBRH3]
29	VTs_CuAlloy	CuCrZr	1.3	147	0.011	0	9.3	0	[XQ7LQV][RWBRH3]

30	VTs_Cu	Cu	6.3	34	0.009	0	9.3	0	[XQ7LQV][RWBRH3]
31	MIX	AISI316	6.3	1	0.01	1	9	0	[XQ7LQV][RWBRH3]
32	Dome	AISI316	6.3	46	0.012	1	5.7	0	[XQ7LQV][RWBRH3]
33	Dome_CuAlloy	CuCrZr	1.3	64	0.02	1	5.7	0	[XQ7LQV][RWBRH3]
34	Cassette_Outlet	AISI316	6.3	771	0.086	1	2.05	0	[XQ7LQV][RWBRH3]
35	CVCSResin	AISI316	12	1	0.01	1	1	0	[XQ7LQV][RWBRH3]
36	CVCSFilter	AISI316	12	1	0.01	1	1	0	[XQ7LQV][RWBRH3]
37	Cold_Linear_Header	AISI316	12	74	0.456	1	5	0	[XQ7LQV][RWBRH3]
38	Btr_blkt	AISI316	12	112	0.174	1	0	0	[XQ7LQV][RWBRH3]
39	Btr_blktr	AISI316	12	110	0.177	1	0	0	[XQ7LQV][RWBRH3]
40	Hot_Linear_Header	AISI316	12	65	0.456	1	5	0	[XQ7LQV][RWBRH3]
41	NHF_FW_fingers_CuAlloy	CuCrZr	1.3	439	0.011	0	2.3	0	[XQ7LQV][RWBRH3]
42	EP	AISI316	6.3	780	0.063	1	1.9	0	[89DGN3]
43	EP_CA	CuCrZr	1.3	131	0.063	1	3.8	0	[89DGN3]
44	EQManifoldin	AISI316	12	45.4	0.364	0	6.6	0	[XQ7LQV][RWBRH3]
45	EQManifoldout	AISI316	12	45.4	0.364	0	6.6	0	[XQ7LQV][RWBRH3]
46	EQRingin	AISI316	12	76	0.254	0	6.8	0	[XQ7LQV][RWBRH3]
47	EQRingout	AISI316	12	86	0.261	0	6.4	0	[XQ7LQV][RWBRH3]
48	EQDistin	AISI316	6.3	234	0.103	0	4.6	0	[XQ7LQV][RWBRH3]
49	EQDistout	AISI316	6.3	234	0.103	0	4.6	0	[XQ7LQV][RWBRH3]
50	UP_CuAlloy	CuCrZr	1.3	41	0.063	1	6	0	[89DGN3]
51a	HXs_HL	AISI316	**2**	2820	0.008	1	2	0	[XQ7LQV][RWBRH3]
51b	HXs_HL2	AISI316	**2**	2820	0.008	1	2	0	[XQ7LQV][RWBRH3]
52	HXs_HL_Box	AISI316	12	28.8	1.741	1	0.26	0	[XQ7LQV][RWBRH3]
53	UManifold_in	AISI316	6.3	959	0.045	0	6.3	0	[XQ7LQV][RWBRH3]
54	UManifold_out	AISI316	6.3	434.633	0.0427	0	7	0	[XQ7LQV][RWBRH3]
55	HXs_CL_Box	AISI316	12	28.8	1.741	1	0.26	0	[XQ7LQV][RWBRH3]
56a	HXs_CL	AISI316	**2**	2820	0.008	1	1.4	0	[XQ7LQV][RWBRH3]
56b	HXs_CL2	AISI316	**2**	2820	0.008	1	1.4	0	[XQ7LQV][RWBRH3]
57	Valves	AISI316	12	46.5	0.206	0	3.3	0	[XQ7LQV][RWBRH3]
58	Valves_r	AISI316	12	46.5	0.248	0	3.8	0	[XQ7LQV][RWBRH3]

Appendix I – IBED PHTS input model GUI

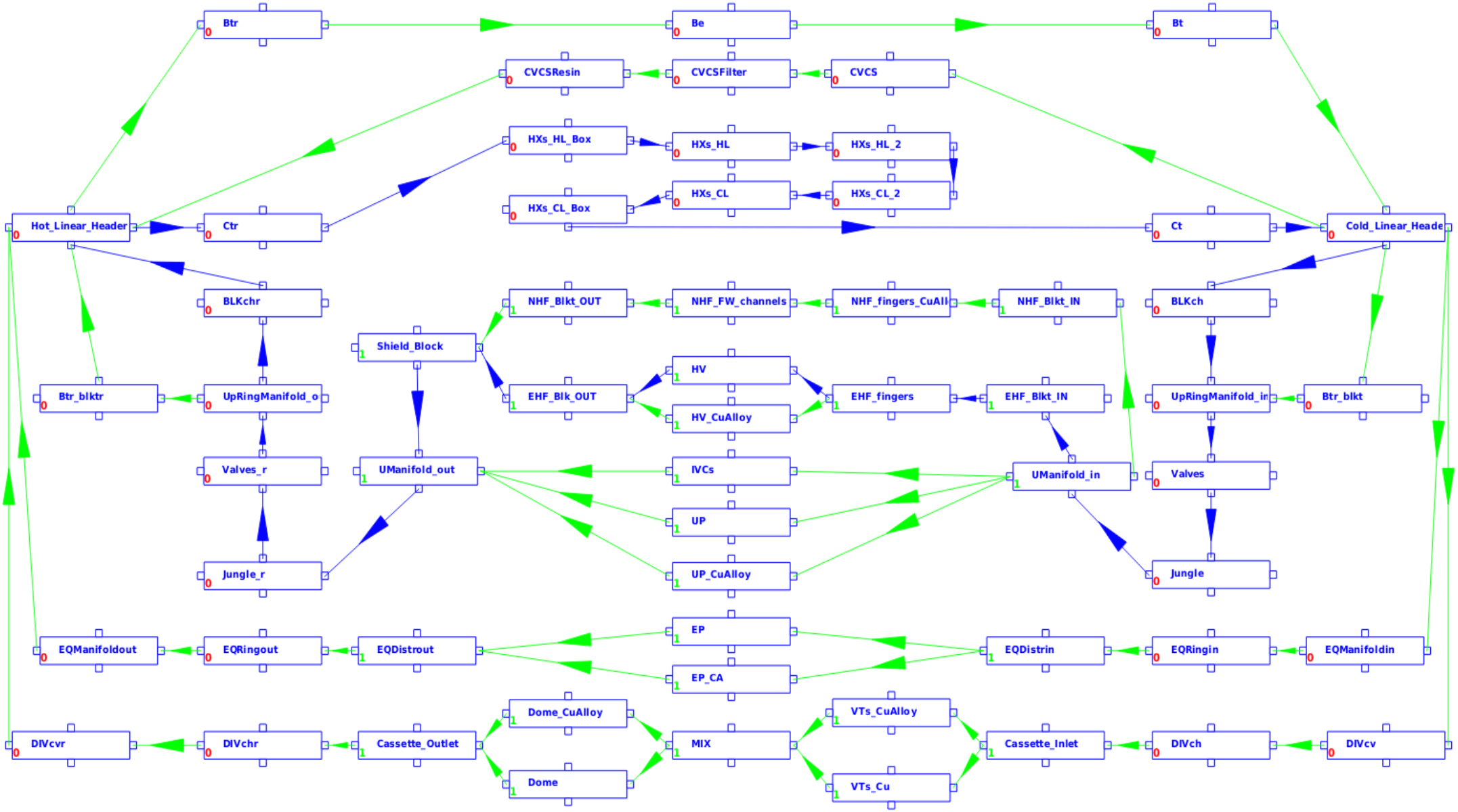

Appendix N – NUCLEO Reaction Rates

Reactions	Finger	Beam	SB Connecting pipes	SB
Cr52(n,p)V52	2.81E-12	9.32E-13	3.99E-13	5.53E-13
Cr53(n,d)V52	1.14E-13	3.41E-14	1.33E-14	2.05E-14
Mn55(n,a)V52	7.68E-13	2.48E-13	1.03E-13	1.47E-13
Cr50(n,g)Cr51	2.27E-10	3.18E-10	2.64E-10	1.64E-10
Cr52(n,2n)Cr51	8.28E-12	2.52E-12	1.00E-12	1.51E-12
Fe54(n,a)Cr51	2.98E-12	9.78E-13	4.15E-13	5.81E-13
Mn55(n,2n)Mn54	2.57E-11	8.11E-12	3.32E-12	4.84E-12
Fe54(n,p)Mn54	1.85E-11	6.86E-12	3.12E-12	4.06E-12
Fe56(n,t)Mn54	5.52E-16	1.58E-16	6.03E-17	9.79E-17
Ni58(n,pa)Mn54	3.99E-15	1.18E-15	4.51E-16	7.03E-16
Mn55(n,g)Mn56	2.18E-10	2.86E-10	2.34E-10	1.52E-10
Fe56(n,p)Mn56	4.09E-12	1.35E-12	5.75E-13	8.02E-13
Fe57(n,d)Mn56	2.34E-13	7.04E-14	2.69E-14	4.27E-14
Co59(n,a)Mn56	1.09E-12	3.82E-13	1.95E-13	2.06E-13
Fe58(n,g)Fe59	2.13E-11	2.63E-11	2.12E-11	1.43E-11
Co59(n,p)Fe59	1.87E-12	6.26E-13	2.69E-13	3.71E-13
Ni62(n,a)Fe59	7.49E-13	2.43E-13	1.02E-13	1.45E-13
Ni58(n,d)Co57	1.91E-11	5.99E-12	2.44E-12	3.58E-12
Co59(n,2n)Co58	6.67E-12	2.09E-12	8.50E-13	1.25E-12
Ni58(n,p)Co58	1.09E-11	4.19E-12	1.94E-12	2.49E-12
Ni60(n,t)Co58	2.86E-16	1.09E-16		6.48E-17

Reactions	Finger	Beam	SB Connecting pipes	SB
Co59(n,g)Co60	**4.49E-10**	**5.19E-10**	**4.10E-10**	**2.94E-10**
Ni60(n,p)Co60	3.14E-12	1.04E-12	4.42E-13	6.17E-13
Ni61(n,d)Co60	2.58E-13	7.76E-14	2.98E-14	4.65E-14
Cu63(n,a)Co60	**1.37E-12**	**4.54E-13**	**1.93E-13**	**2.71E-13**
Ni58(n,2n)Ni57	7.48E-13	2.26E-13	8.94E-14	1.36E-13
Fe54(n,g)Fe55	3.33E-11	4.56E-11	3.76E-11	2.37E-11
Fe56(n,2n)Fe55	1.30E-11	4.03E-12	1.62E-12	2.41E-12
Ni58(n,a)Fe55	4.00E-12	1.37E-12	6.00E-13	8.13E-13
Ni58(n,g)Ni59	6.66E-11	9.26E-11	7.66E-11	4.77E-11
Ni60(n,2n)Ni59	1.18E-11	3.62E-12	1.45E-12	2.17E-12
Ni62(n,g)Ni63	2.04E-10	2.84E-10	2.35E-10	1.46E-10
Ni64(n,2n)Ni63	3.07E-11	9.73E-12	4.00E-12	5.80E-12
Cu63(n,p)Ni63	3.21E-12	1.25E-12	5.82E-13	7.47E-13
Cu63(n,2n)Cu62	1.44E-11	4.47E-12	1.80E-12	2.67E-12
Cu63(n,g)Cu64	8.10E-11	1.01E-10	8.11E-11	5.48E-11
Cu65(n,2n)Cu64	2.92E-11	9.22E-12	3.78E-12	5.50E-12
Cu65(n,g)Cu66	3.77E-11	4.76E-11	3.85E-11	2.57E-11
Ag107(n,g)Ag108m*	1.05E-11	1.12E-11	8.67E-12	6.55E-12
Ag109(n,2n)Ag108m*	2.21E-11	7.04E-12	2.90E-12	4.19E-12
Cd108(n,p)Ag108m*	4.71E-13	2.69E-13		1.59E-13
Zr92(n,g)Zr93	7.17E-12	6.88E-12	5.16E-12	4.23E-12
Zr94(n,2n)Zr93	5.09E-11	1.65E-11	6.95E-12	9.82E-12
Zr94(n,g)Zr95	2.90E-12	2.34E-12	1.64E-12	1.59E-12
Zr96(n,2n)Zr95	5.28E-11	1.72E-11	7.23E-12	1.02E-11

*Ag108m not considered in OSCAR calculation

Appendix O – ACPs contribution to the ORE

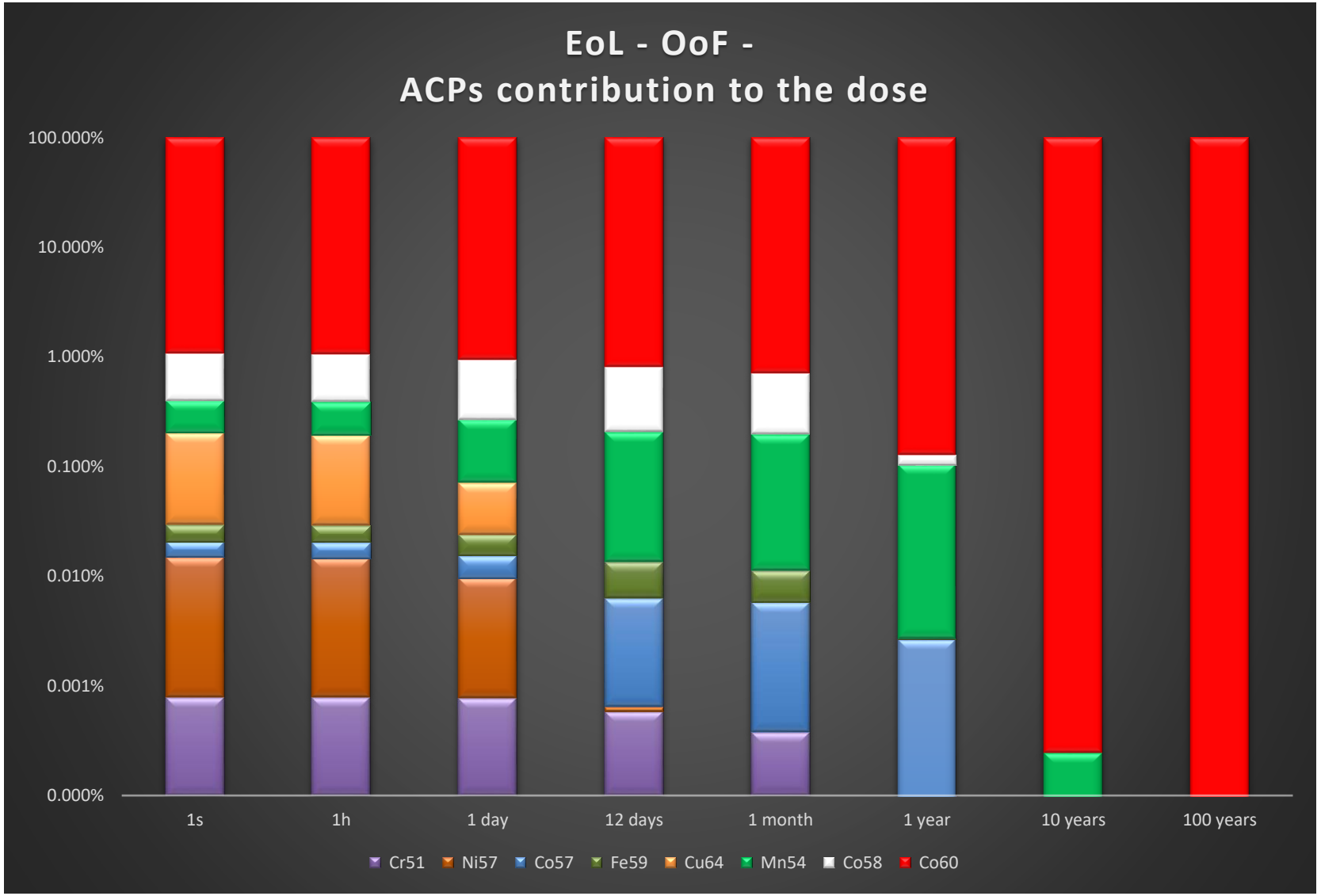

Appendix V – Inputs Independent Verification from CEA

	Name	Father Input(s)	Change	Comment	CEA REVIEW
1	i9	i8	Roughness for AISI IF materials have been changed from 12 to 6.3 (as already used for DIV) also for Upper and Equatorial clients	REFERENCE CASE for VALIDATION REPORT	OK
2	i90	i9 – i80	Simplified version of the i9 input: only gamma emitters considered in NUCLEO and no printing during dwell time periods.		OK
3	i90_h0	i90	H2 concentration set to 0 ml/kgw	i90 H2 concentration @ 25 ml/kgw Doesn't work because of the H2=0 error	OK
4	i90_h5	i90	H2 concentration set to 5 ml/kgw	i90 H2 concentration @ 25 ml/kgw	OK
5	i90_h15	i90	H2 concentration set to 15 ml/kgw	i90 H2 concentration @ 25 ml/kgw	OK
6	i90_h25	i90	H2 concentration set to 15 ml/kgw	i90 H2 concentration @ 25 ml/kgw not reported here	OK
7	i90_h35	i90	H2 concentration set to 15 ml/kgw	i90 H2 concentration @ 25 ml/kgw not reported here	OK
8	i90_h40	i90	H2 concentration set to 40 ml/kgw	i90 H2 concentration @ 25 ml/kgw	OK
9	i90_h60	i90	H2 concentration set to 60 ml/kgw	i90 H2 concentration @ 25 ml/kgw	OK
10	i90_NL	i90	Lithium concentration set to 0 ALWAYS	No pH control simulated	OK
11	i90_LB	i90	Lithium injection limited to baking operation	pH control only during baking	OK

12	i90_LPO	i90	Lithium injection limited to dwell-burn operations	pH control only during dwell-burn operations	OK
13	i90_NoBake	i90	No water baking		OK for Temperatures – Pressure could be reduced
14	i90_lowbake	i90	Baking flow rate reduced to 1% of the nominal flow rate (factor 10 reduction)	Flow rate during baking of 52 kg/s instead of 516	OK
15	i90_CV10	i90	CVCS flow rate increased to 10% of the nominal flow rate (factor 10 increase) during baking	Arbitrary reduction of the flow rate in the DIV and EQ regions to compensate the CVCS increase	OK?
16	i90_JRR	i90	Jungle Gym regions with reduced roughness (2microns instead of 12)		OK
17	i90_NoCoIF	i90	In-flux components simulated without Co (AISI 6 microns, Cu, CuCrZr) and Cu63 (n,alpha) and Ni60 (n,p) reactions removed	not reported here	OK
18	i90_MCo20	i90	FW-BLK manifolds with increased Co content (2000 ppm instead of 500)	Required to justify Deviation Requests on cobalt content increase for FW-BLK elbows and fittings – not reported here	OK